# Supplementary Information

## Ferrocene functionalized dithiocarbamate complexes holding thiophene arms: Synthesis, crystal structure, electrochemical, *in silico* interaction profiling, and apoptosis induction in HeLa Cells

Bhaveshkumar B. Makwana[a], Heena A. Parmar[b], Adam N. Khan[c], José M. Padrón[c], and Umesh P. Tarpada[d]*

[a] Department of Chemistry, School of Sciences, Gujarat University, Ahmedabad- 380009, Gujarat, India.

[b] Department of Chemistry, Gujarat Arts and Science College, Ahmedabad- 380006, Gujarat, India.

[c] BioLab, Instituto Universitario de Bio-Orgánica "Antonio González", Universidad de la Laguna, C/ Astrofísico Francisco Sánchez 2, 38206 La Laguna, Spain.

[d] Department of Chemistry, Government Arts and Science College, Bavla, Ahmedabad-382220, Gujarat, India.

***Corresponding author:** umeshtarpada@gmail.com (U.P. Tarpada)

**Contents in Supporting Information**


| # | Content | Page |
|---|---|---|
| | **Experimental data of ligands $L^1$ & $L^2$** | |
| - | General procedure and experimental data of **$L^1$** & **$L^2$** | 3-4 |
| | **Spectral characterization (NMR, FT-IR & ESI-MS)** | |
| Fig. S1 | $^1$H NMR spectra (400 MHz, DMSO-$d_6$) of ligand **$L^1$**. | 5-5 |
| Fig. S2 | $^{13}$C{$^1$H} NMR spectra (400 MHz, DMSO-$d_6$) of ligand **$L^1$**. | 5-5 |
| Fig. S3 | $^1$H NMR spectra (400 MHz, DMSO-$d_6$) of ligand **$L^2$**. | 6-6 |
| Fig. S4 | $^{13}$C{$^1$H} NMR spectra (400 MHz, DMSO-$d_6$) of ligand **$L^2$**. | 6-6 |
| Fig. S5 | $^1$H NMR spectra (400 MHz, DMSO-$d_6$) of complex **1**. | 7-7 |
| Fig. S6 | $^{13}$C{$^1$H} NMR spectra (400 MHz, DMSO-$d_6$) of complex **1**. | 7-7 |
| Fig. S7 | $^1$H NMR spectra (400 MHz, DMSO-$d_6$) of complex **3**. | 8-8 |
| Fig. S8 | $^{13}$C{$^1$H} NMR spectra (400 MHz, DMSO-$d_6$) of complex **3**. | 8-8 |
| Fig. S9 | $^1$H NMR spectra (400 MHz, DMSO-$d_6$) of complex **4**. | 9-9 |
| Fig. S10 | $^{13}$C{$^1$H} NMR spectra (400 MHz, DMSO-$d_6$) of complex **4**. | 9-9 |
| Fig. S11 | $^1$H NMR spectra (400 MHz, DMSO-$d_6$) of complex **6**. | 10-10 |
| Fig. S12 | $^{13}$C{$^1$H} NMR spectra (400 MHz, DMSO-$d_6$) of complex **6**. | 10-10 |

| | | |
|---|---|---|
| Fig. S13 | FT-IR spectra of ligand $\mathbf{L^1}$. | 11-11 |
| Fig. S14 | FT-IR spectra of ligand $\mathbf{L^2}$. | 11-11 |
| Fig. S15 | FT-IR spectra of complex **1**. | 12-12 |
| Fig. S16 | FT-IR spectra of complex **2**. | 12-12 |
| Fig. S17 | FT-IR spectra of complex **3**. | 13-13 |
| Fig. S18 | FT-IR spectra of complex **4**. | 13-13 |
| Fig. S19 | FT-IR spectra of complex **5**. | 14-14 |
| Fig. S20 | FT-IR spectra of complex **6**. | 14-14 |
| Fig. S21 | ESI-MS spectra of complex **1**. | 15-15 |
| Fig. S22 | ESI-MS spectra of complex **2**. | 15-15 |
| Fig. S23 | ESI-MS spectra of complex **3**. | 15-15 |
| Fig. S24 | ESI-MS spectra of complex **4**. | 15-15 |
| Fig. S25 | ESI-MS spectra of complex **5**. | 16-16 |
| Fig. S26 | ESI-MS spectra of complex **6**. | 16-16 |
| **UV-visible study** | | |
| Table S1 | UV-visible absorption data of ligand precursors and complexes **1-6** in $10^{-5}$ DCM. | 17-17 |
| **DFT study** | | |
| Table S2 | Summary of computational (DFT) data for complexes **1-6.** | 18-18 |
| **Cyclic voltammetry study** | | |
| Table S3 | Electrochemical parameters derived from the voltammograms for ligands $\mathbf{L^1}$-$\mathbf{L^2}$ and complexes (**1-6**). | 19-19 |
| **TGA data** | | |
| Table S4 | Thermogravimetric data of dithiocarbamate metal complexes **1-6**. | 20-20 |
| **Anticancer activity** | | |
| Table S5 | *In vitro* anticancer activity of synthesized ligands $\mathbf{L^1}$, $\mathbf{L^2}$, and complexes **1-6**. | 21-21 |
| **Docking study** | | |
| Fig. S27 | Molecular docking studies of 5-fluorouracil (5-FU) with 3qx3. | 22-22 |
| Fig. S28 | Molecular docking studies of co-ligand (native) with 3qx3. | 22-22 |
| Fig. S29 | Molecular docking studies of complex **1** with 3qx3. | 23-23 |
| Fig. S30 | Molecular docking studies of complex **2** with 3qx3. | 23-23 |
| Fig. S31 | Molecular docking studies of complex **4** with 3qx3. | 24-24 |
| Fig. S32 | Molecular docking studies of complex **5** with 3qx3. | 24-24 |
| Fig. S33 | Molecular docking studies of 5-fluorouracil (5-FU) with 4jps. | 25-25 |
| Fig. S34 | Molecular docking studies of co-ligand (native) with 4jps. | 25-25 |
| Fig. S35 | Molecular docking studies of complex **1** with 4jps. | 26-26 |
| Fig. S36 | Molecular docking studies of complex **2** with 4jps. | 26-26 |
| Fig. S37 | Molecular docking studies of complex **4** with 4jps. | 27-27 |
| Fig. S38 | Molecular docking studies of complex **5** with 4jps. | 27-27 |

*General procedure for the syntheses of* ***L*$^{1}$*/L*$^{2}$ *ligands***

An equivalent amount of *formyl ferrocene* (0.137 g, 1 mmol) was added to a solution containing thiophenemethylamine (0.122 g, 1 mmol) or thiopheneethylamine (0.172 g, 1 mmol) in absolute alcohol (10 mL) at room temperature. After five hours of stirring of the reaction mixture, thin layer chromatography (TLC) was used to verify that the completion of reaction. The reaction mixture was filtered through a celite pad, dried over $Na_2SO_4$, and the solvent was extracted under vacuum to reveal the ligands **L$^{1}$** and **L$^{2}$**.

*N*-thiophenemethyl-*N*-methylferrocenylamine (**L$^{1}$**)

M.W. 311.22; Reddish brown solid; Yield: *ca* 281.0 mg, 90.3%; m.p. 159-163 °C dec. $^{1}$H NMR (400 MHz, DMSO-$d_6$) δ ppm: 7.39-7.37 (m, 1H, Th*H*-5); 6.98-6.96 (m, 2H, Th*H*-3 & Th*H*-4); 4.20-4.18 (m, 2H, Fc); 4.12 (s, 7H, Fc); 4.09-4.08 (m, 2H, -C$H_2$Th); 3.87 (s, 2H, -C$H_2$Fc). $^{13}$C{$^{1}$H} NMR (400 MHz, DMSO-$d_6$) δ ppm: 144.7, 127.1, 125.9, 125.6, 125.3, 125.2, 118.5, 86.5, 70.2, 68.8, 68.1, 67.8, 47.4 (-*C*H$_2$Fc), 47.2 (-*C*H$_2$Th). Infrared spectrum (KBr disc, cm$^{-1}$): 3922 w, 3321 w (*v*(N-H)), 3086 s (aromatic, *v*(C-H)), 2813 s (arylidene, *v*(C-H)), 1634 m, 1438 s (*v*(C=N)), 1328 w, 1227 m, 1101 s, 1038 m (*v*(C-C)), 997 m, 923 w, 813 s, 697 s (aromatic out-of-plane bending, γ(C-H))/(thiophene *v*(C-S)), 611 m, 482 s (*v*(Fe-Cp)), 415 w. UV-visible (DCM, *λ*, nm): 306, 272.

*N*-thiopheneethyl-*N*-methylferrocenylamine (**L$^{2}$**)

M.W. 325.25; Reddish brown solid; Yield: *ca* 291.7 mg, 89.7%; m.p. 163-168 °C dec. $^{1}$H NMR (400 MHz, DMSO-$d_6$) δ ppm: 7.33 (m, 1H, Th*H*-5); 6.96-6.91 (m, 2H, Th*H*-3 & Th*H*-4); 4.21 (s, 2H, Fc); 4.09 (s, 7H, Fc); 3.48 (s, 2H, -CH$_2$C$H_2$Th); 2.98 (s, 2H, -C$H_2$Fc); 2.84 (s, 2H, -C$H_2$CH$_2$Th). $^{13}$C{$^{1}$H} NMR (400 MHz, DMSO-$d_6$) δ ppm: 143.4, 142.9, 127.3, 127.0, 125.5, 125.1, 124.3, 124.1, 87.0, 83.3, 73.1, 70.2, 69.3, 68.7, 68.6, 68.0, 67.9, 67.7, 59.6, 52.6, 50.8 (-*C*H$_2$Fc), 50.2, 48.2 (-*C*H$_2$Th), 30.0, 27.6. Infrared spectrum (KBr disc, cm$^{-1}$):

3813 w, 3640 w ($\nu$(N-H)), 3086 s (aromatic, $\nu$(C-H)), 2915 w, 2815 s (arylidene, $\nu$(C-H)), 2250 w, 1641 m, 1438 s ($\nu$(C=N)), 1321 w, 1229 m, 1104 s ($\nu$(C-C)), 998 m, 920 m, 814 s, 692 s (aromatic out-of-plane bending, $\gamma$(C-H))/(thiophene $\nu$(C-S)), 480 s ($\nu$(Fe-Cp)), 409 w. UV-visible (DCM, $\lambda$, nm): 318, 270.

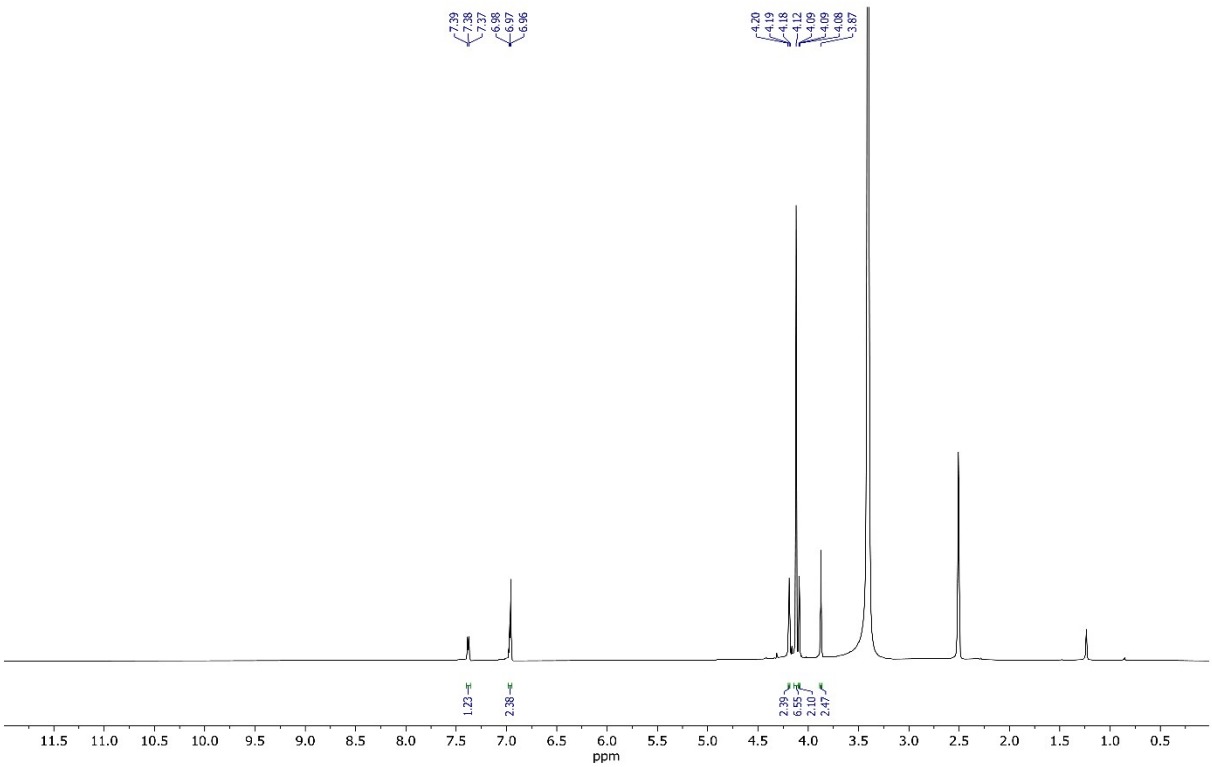


**Fig. S1.** $^{1}$H NMR spectra (400 MHz, DMSO-$d_6$) of ligand **L$^{1}$**.

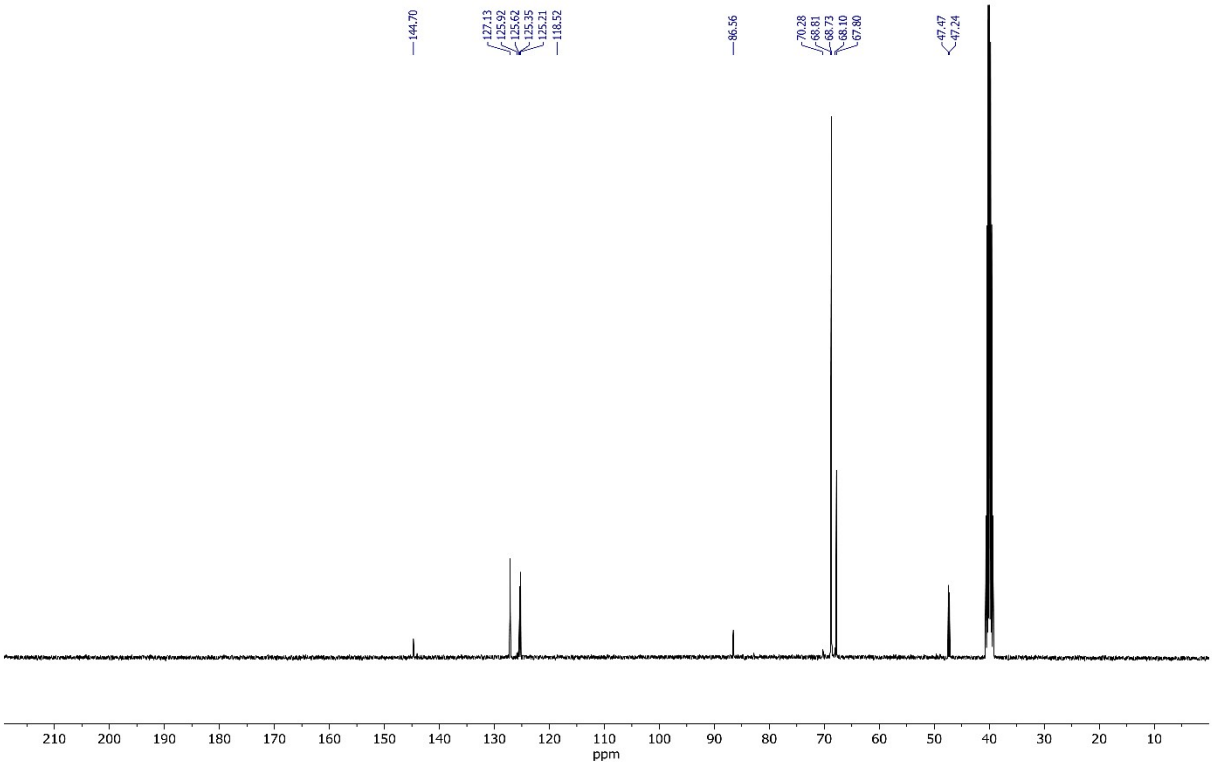


**Fig. S2.** $^{13}$C{$^{1}$H} NMR spectra (400 MHz, DMSO-$d_6$) of ligand **L$^{1}$**.

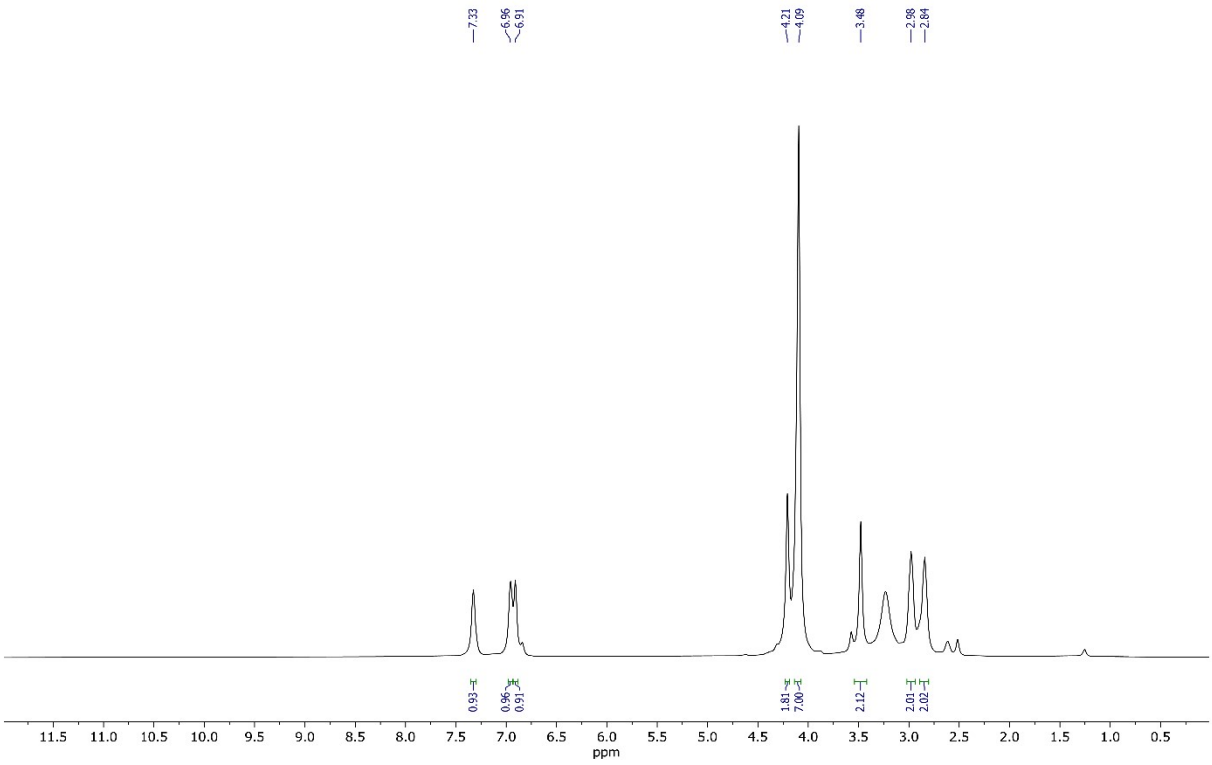


**Fig. S3.** $^{1}$H NMR spectra (400 MHz, DMSO-$d_6$) of ligand **L²**.

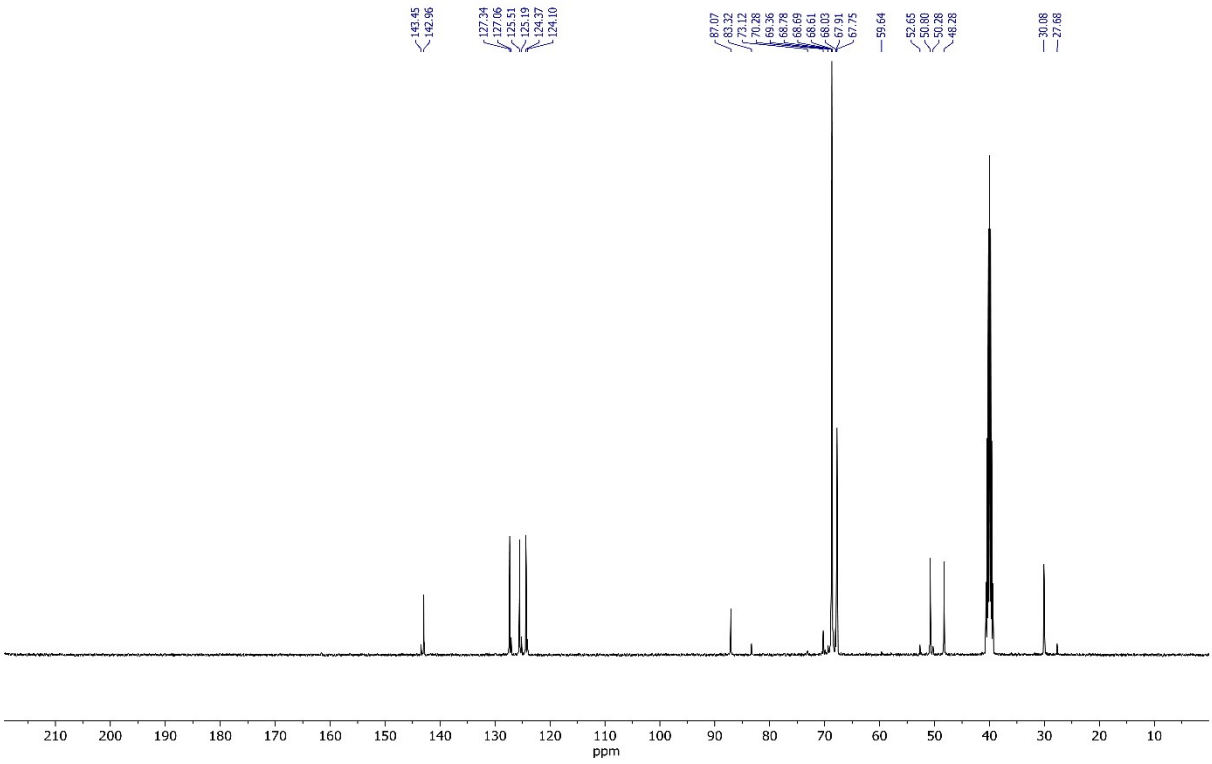


**Fig. S4.** $^{13}$C{$^{1}$H} NMR spectra (400 MHz, DMSO-$d_6$) of ligand **L²**.

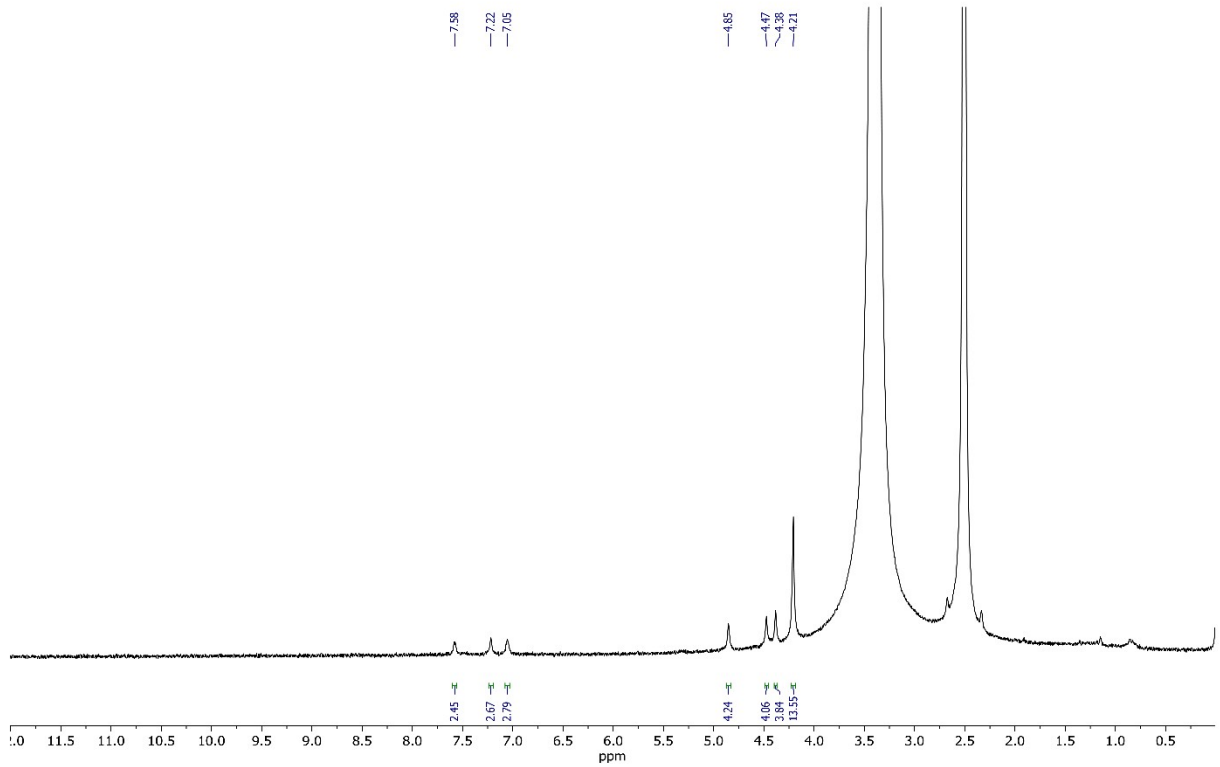


**Fig. S5.** $^{1}H$ NMR spectra (400 MHz, DMSO-$d_6$) of complex **1**.

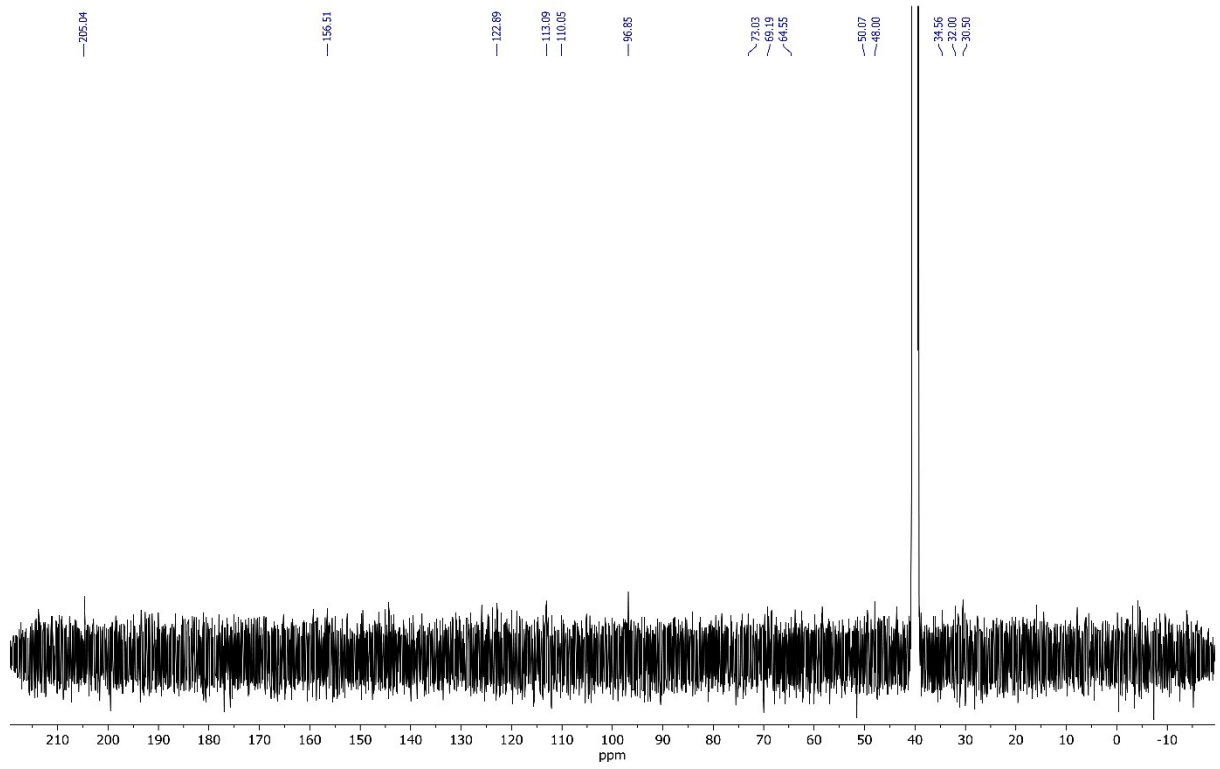


**Fig. S6.** $^{13}C\{^{1}H\}$ NMR spectra (400 MHz, DMSO-$d_6$) of complex **1**.

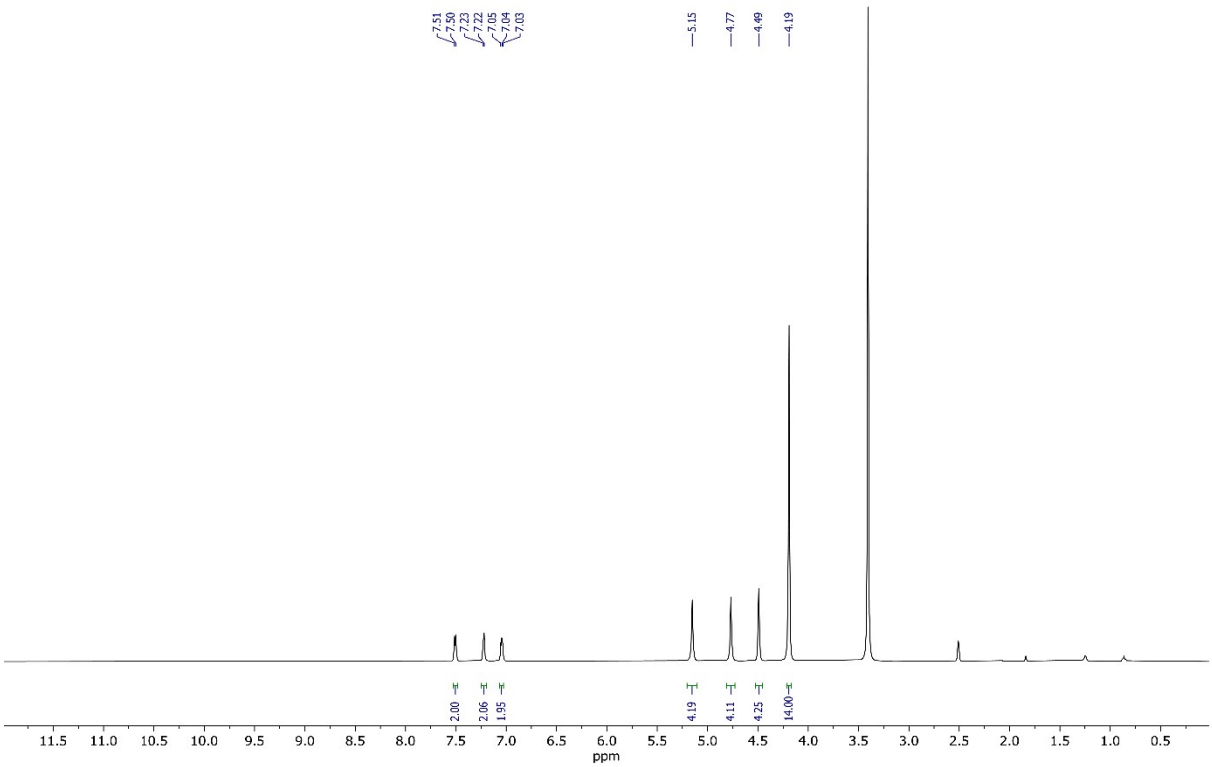


**Fig. S7.** $^{1}H$ NMR spectra (400 MHz, DMSO-$d_6$) of complex **3**.

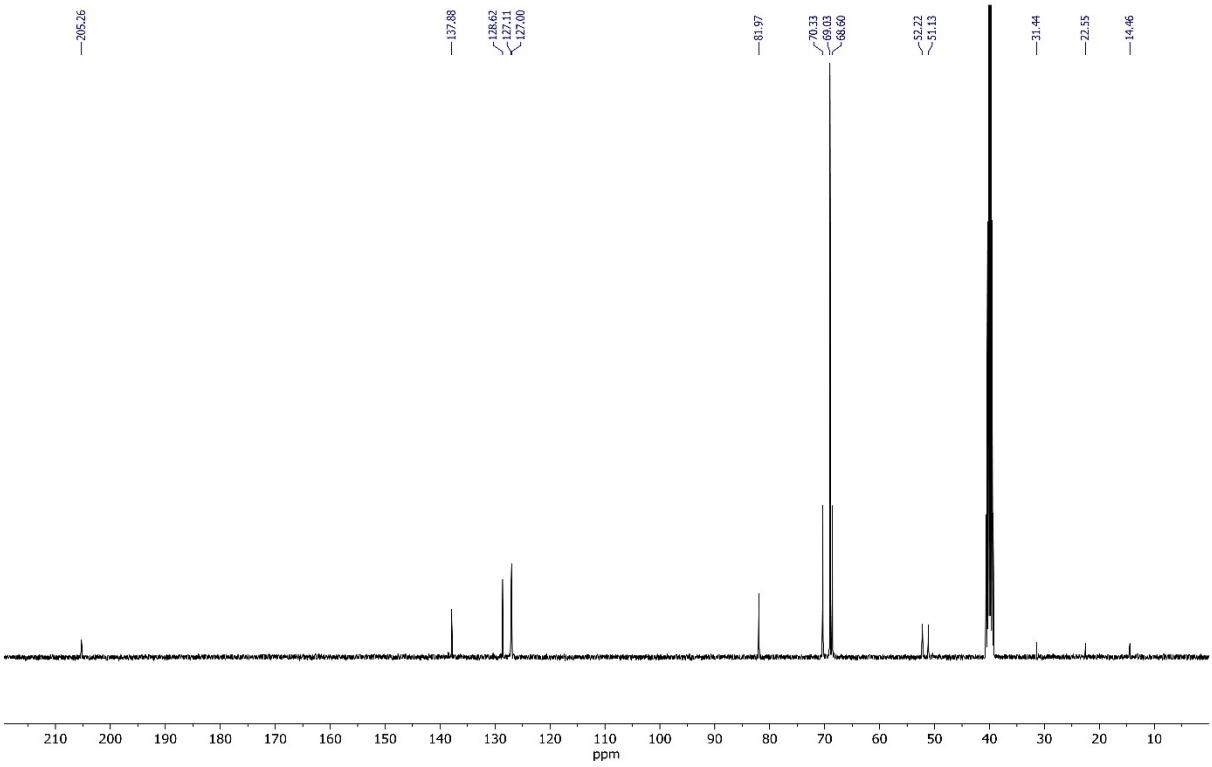


**Fig. S8.** $^{13}C\{^{1}H\}$ NMR spectra (400 MHz, DMSO-$d_6$) of complex **3**.

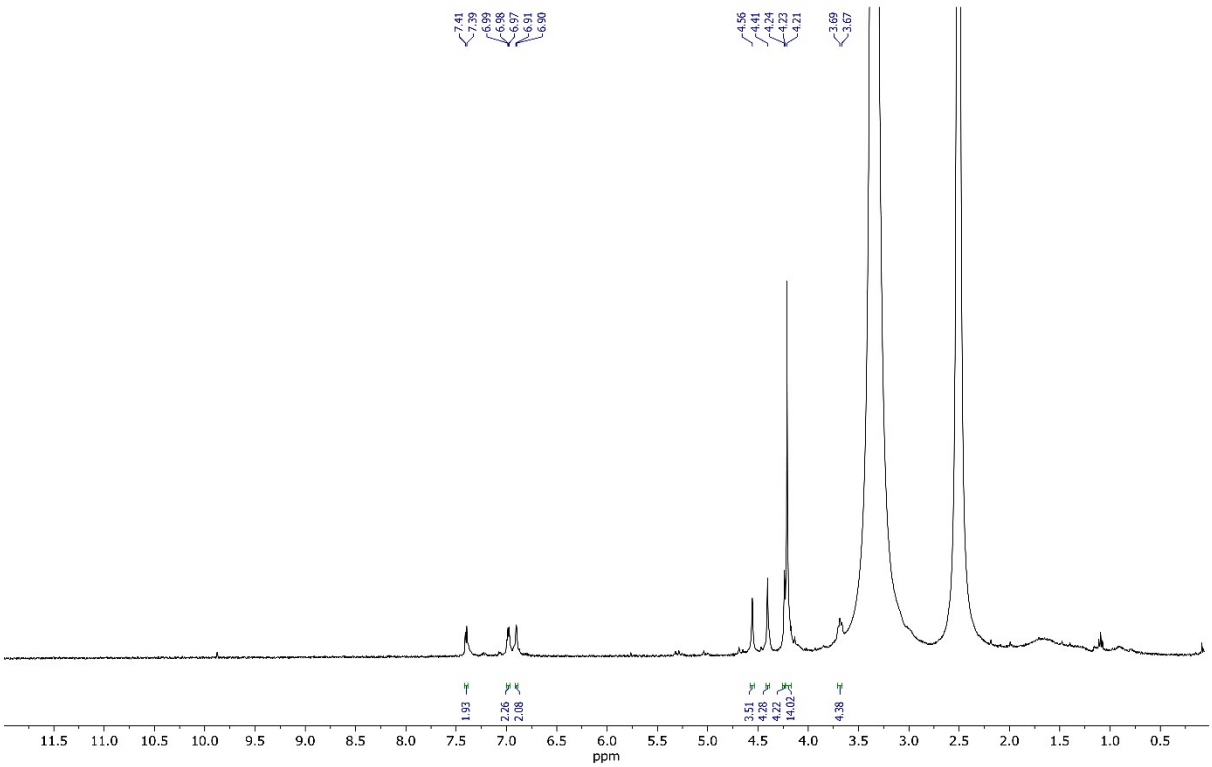


**Fig. S9.** $^{1}$H NMR spectra (400 MHz, DMSO-$d_6$) of complex **4**.

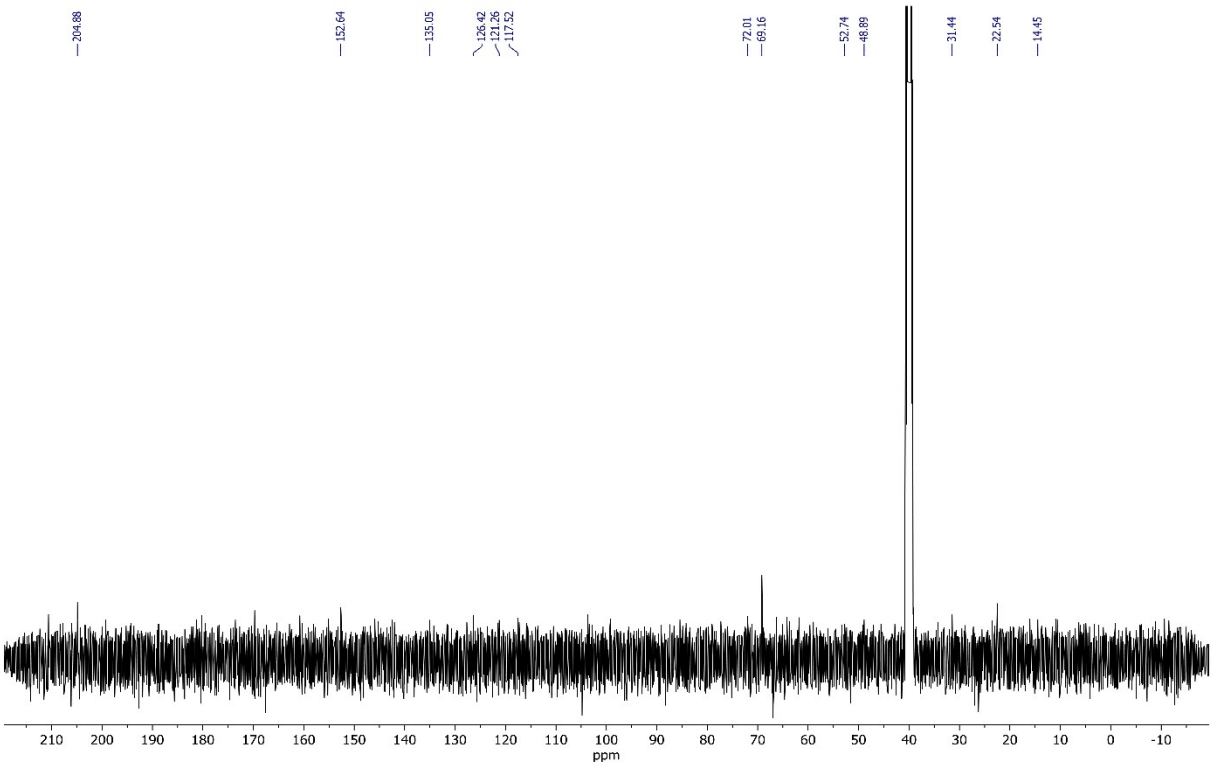


**Fig. S10.** $^{13}$C{$^{1}$H} NMR spectra (400 MHz, DMSO-$d_6$) of complex **4**.

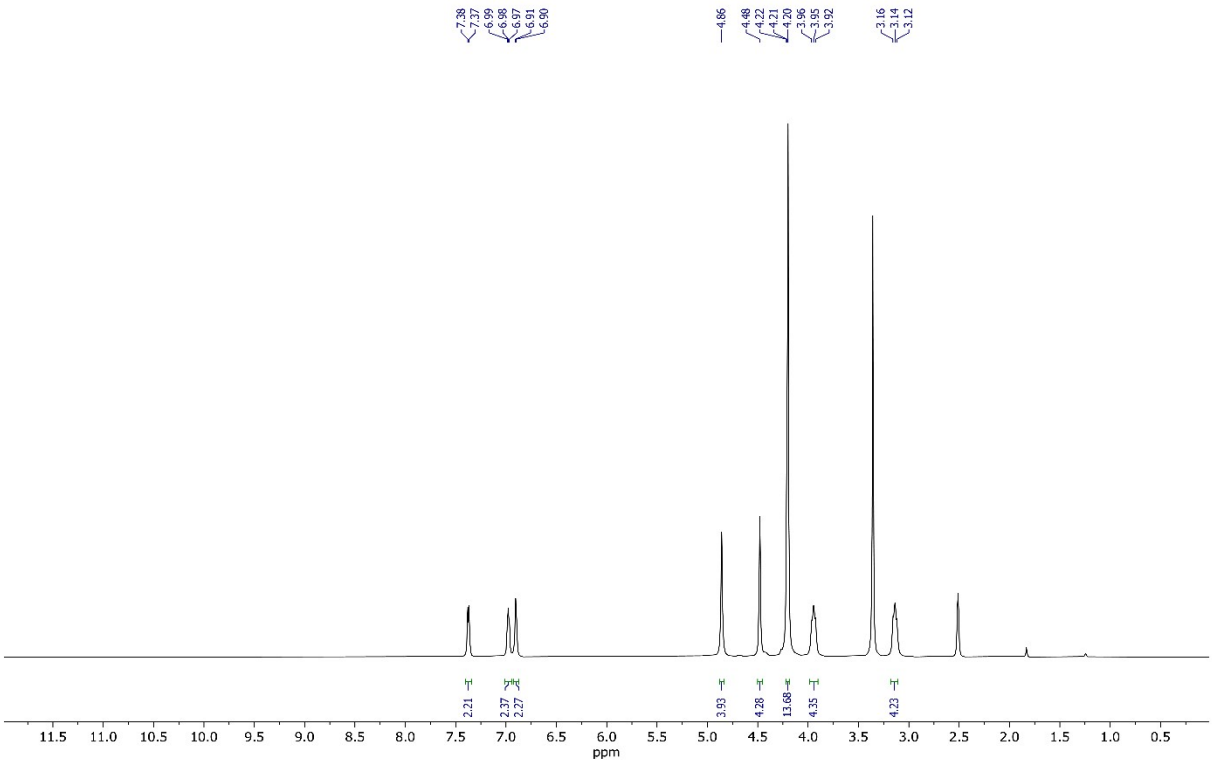


**Fig. S11.** $^{1}$H NMR spectra (400 MHz, DMSO-$d_6$) of complex **6**.

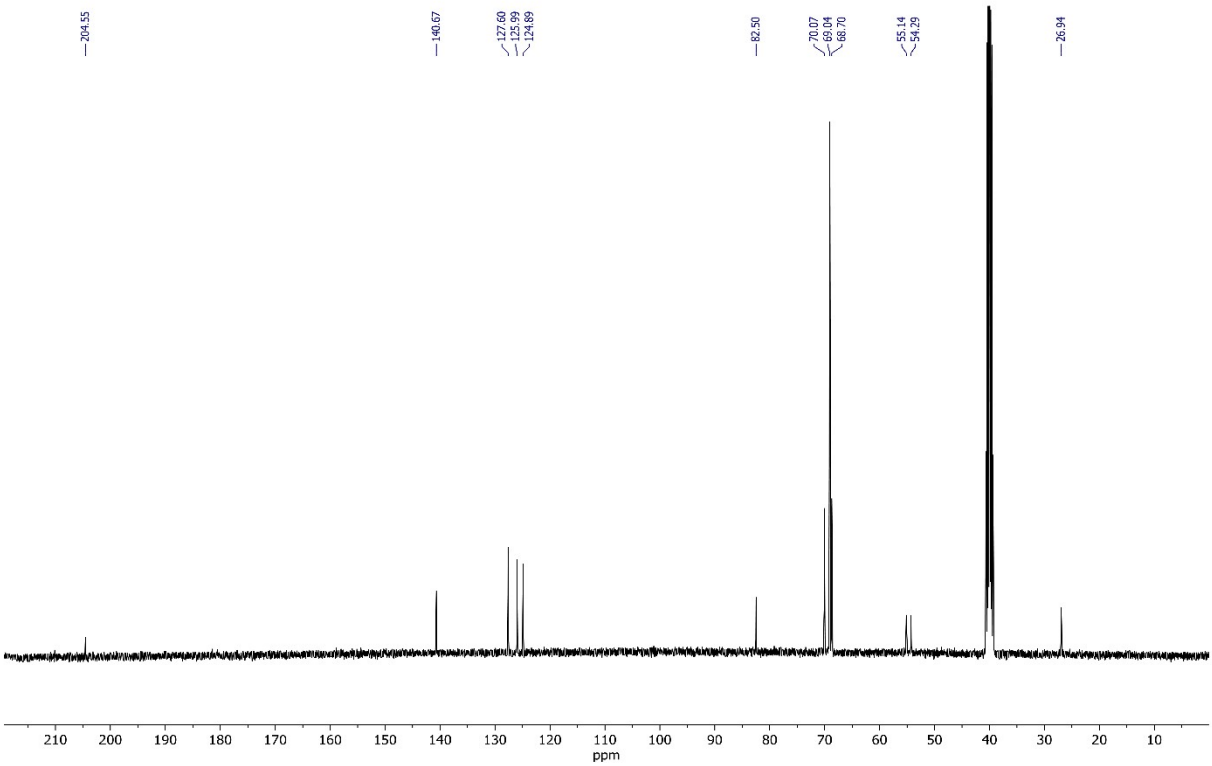


**Fig. S12.** $^{13}$C{$^{1}$H} NMR spectra (400 MHz, DMSO-$d_6$) of complex **6**.

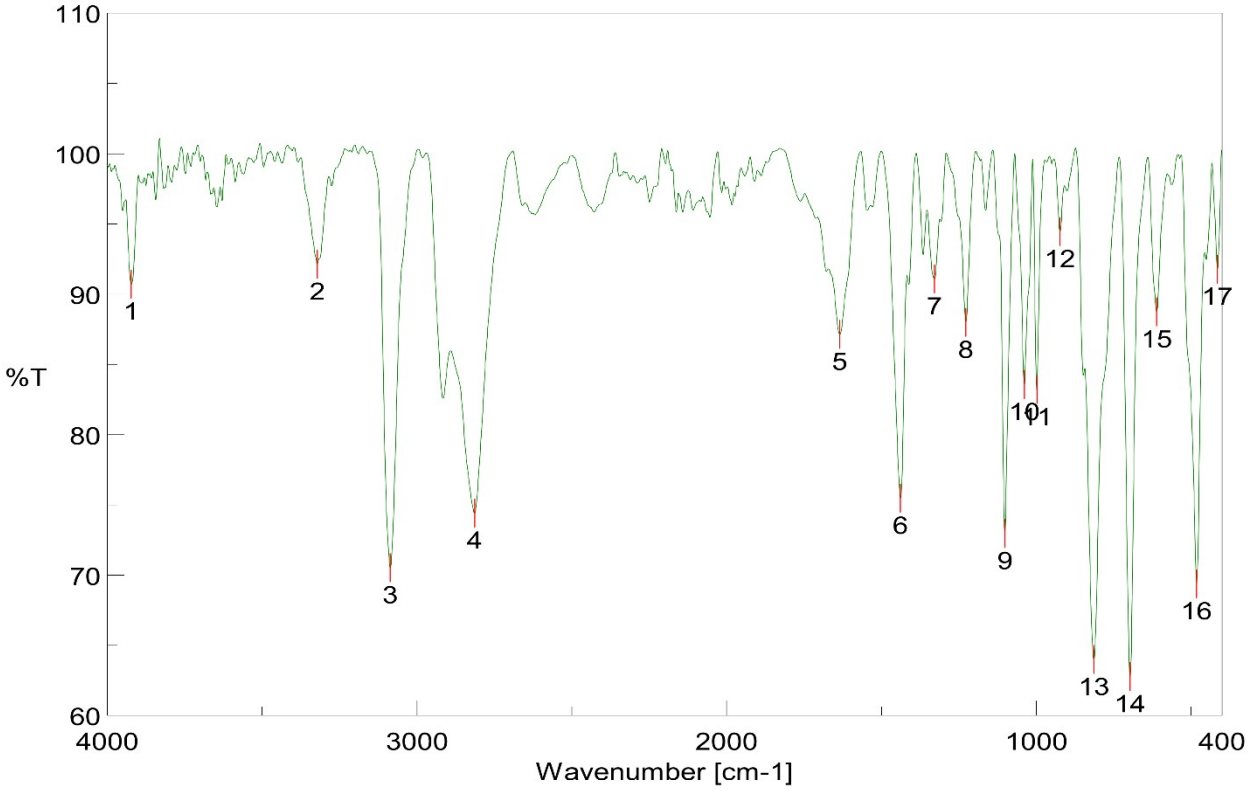


**Fig. S13.** FT-IR spectra of ligand $\mathbf{L^1}$.

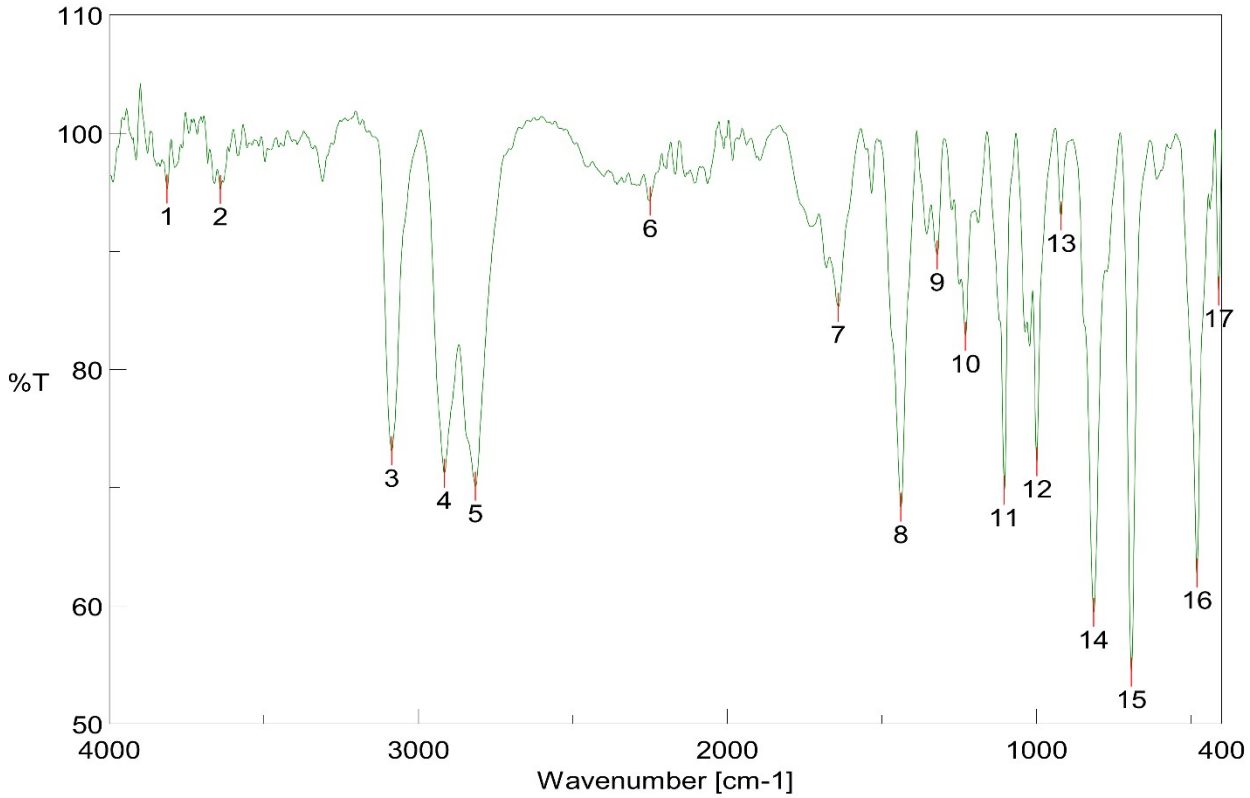


**Fig. S14.** FT-IR spectra of ligand $\mathbf{L^2}$.

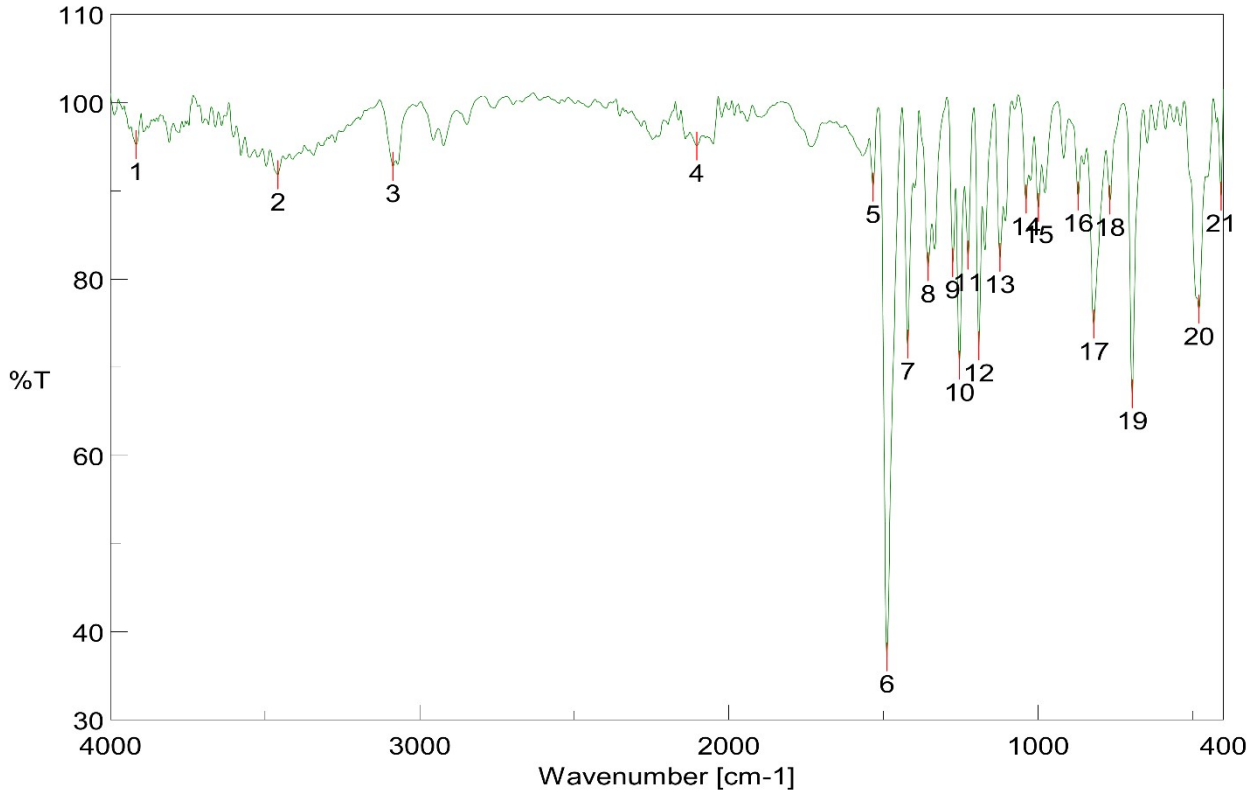


**Fig. S15.** FT-IR spectra of complex **1**.

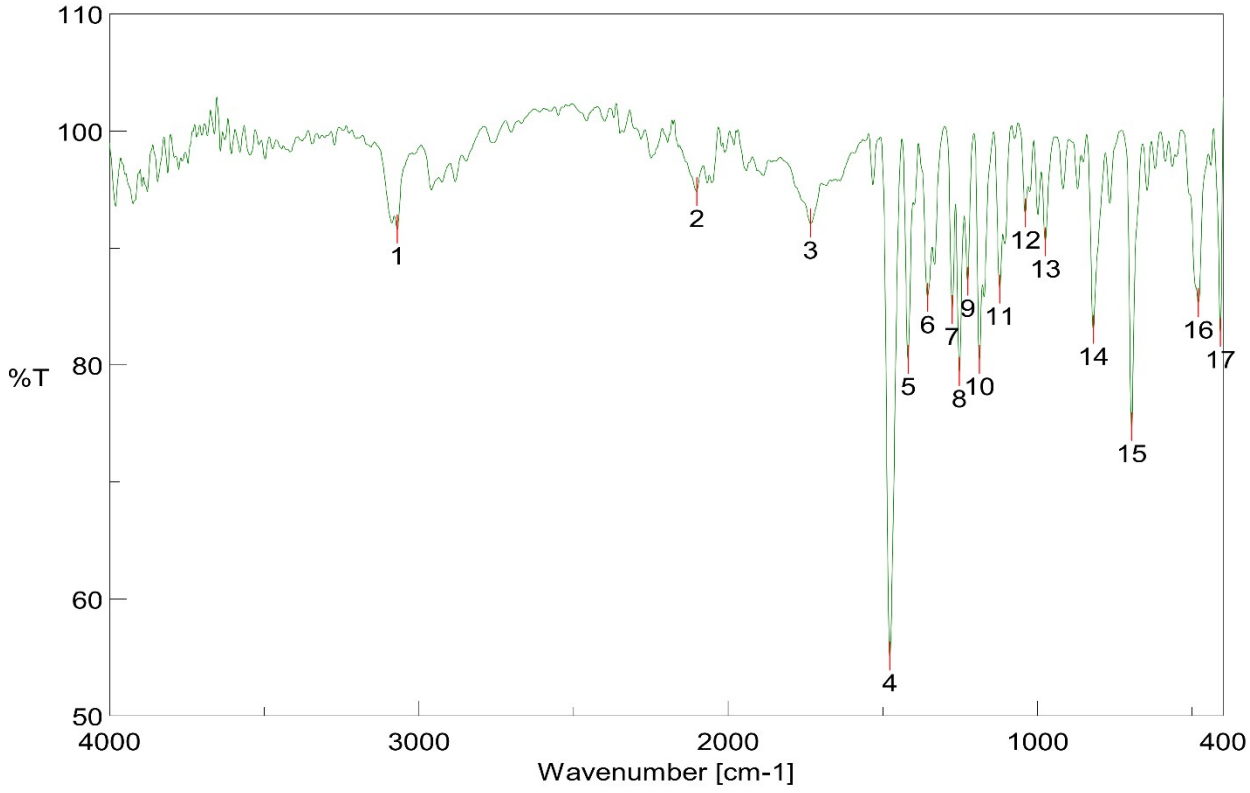


**Fig. S16.** FT-IR spectra of complex **2**.

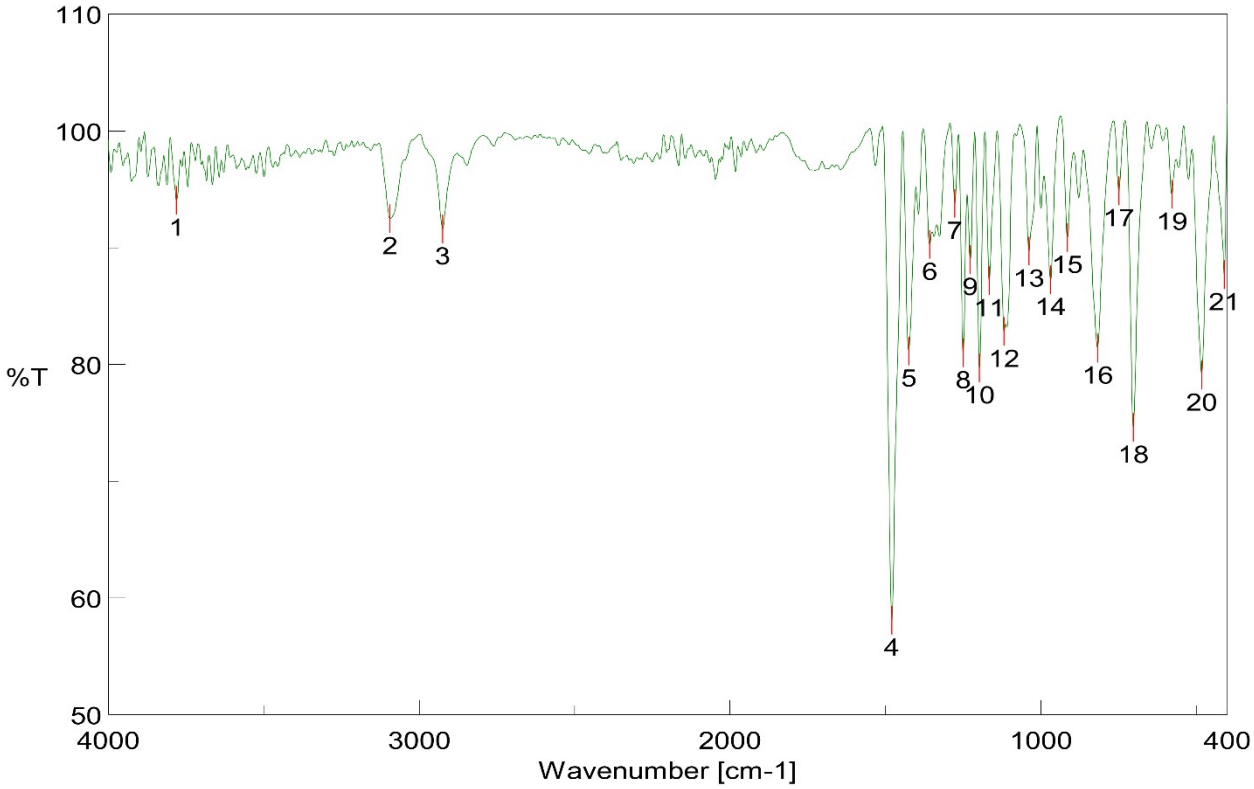


**Fig. S17.** FT-IR spectra of complex **3**.

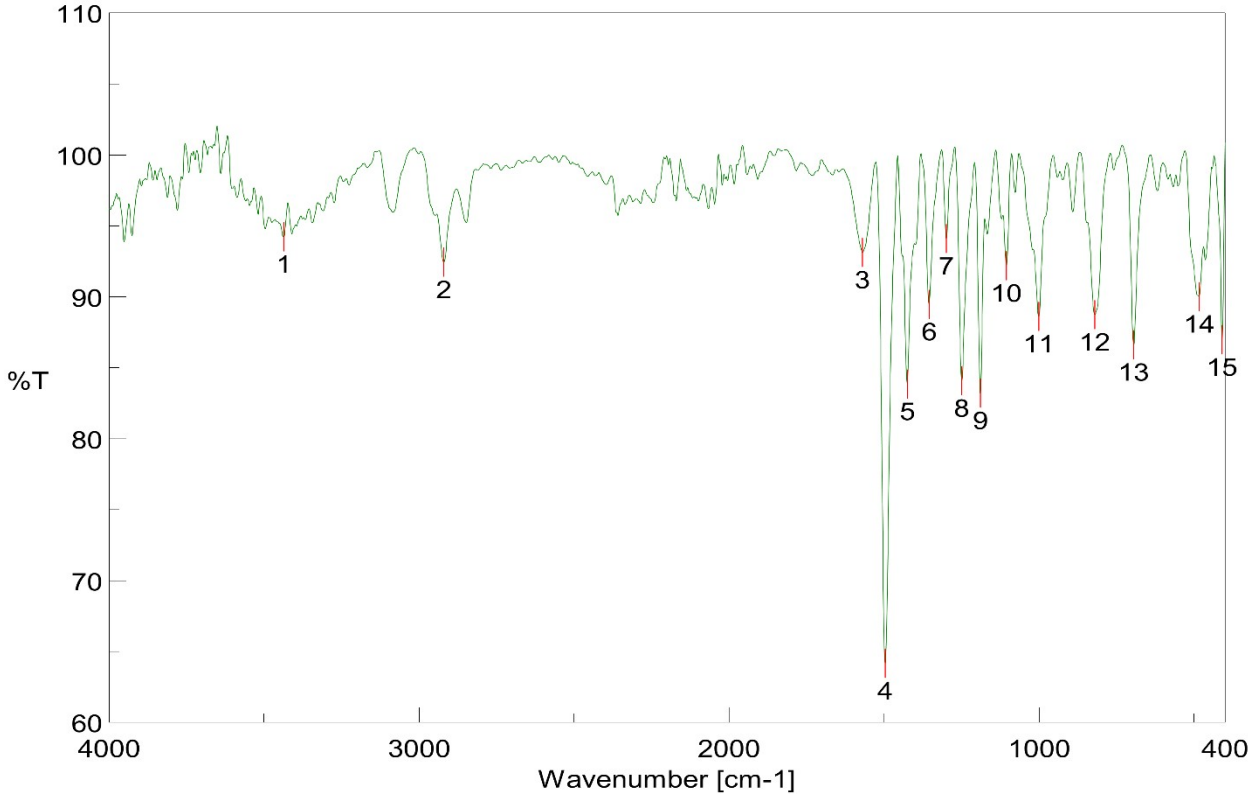


**Fig. S18.** FT-IR spectra of complex **4**.

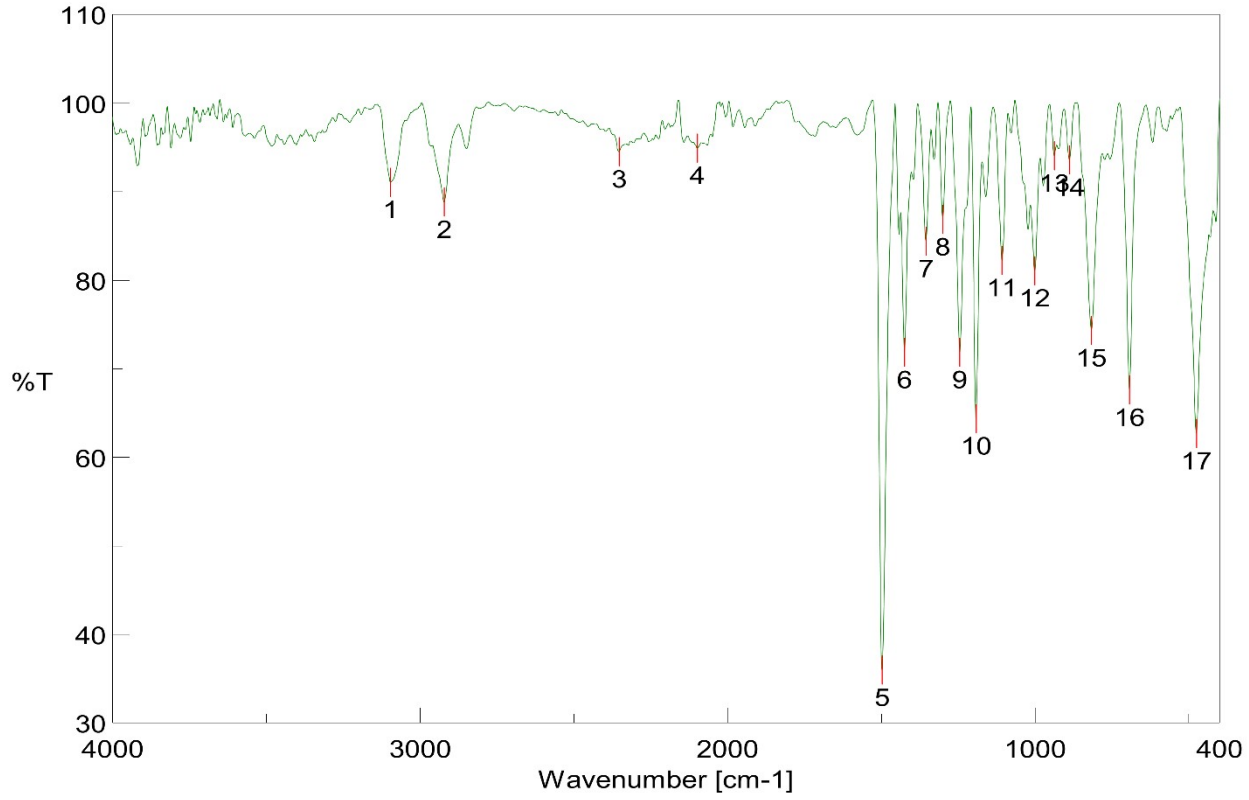


**Fig. S19.** FT-IR spectra of complex **5**.

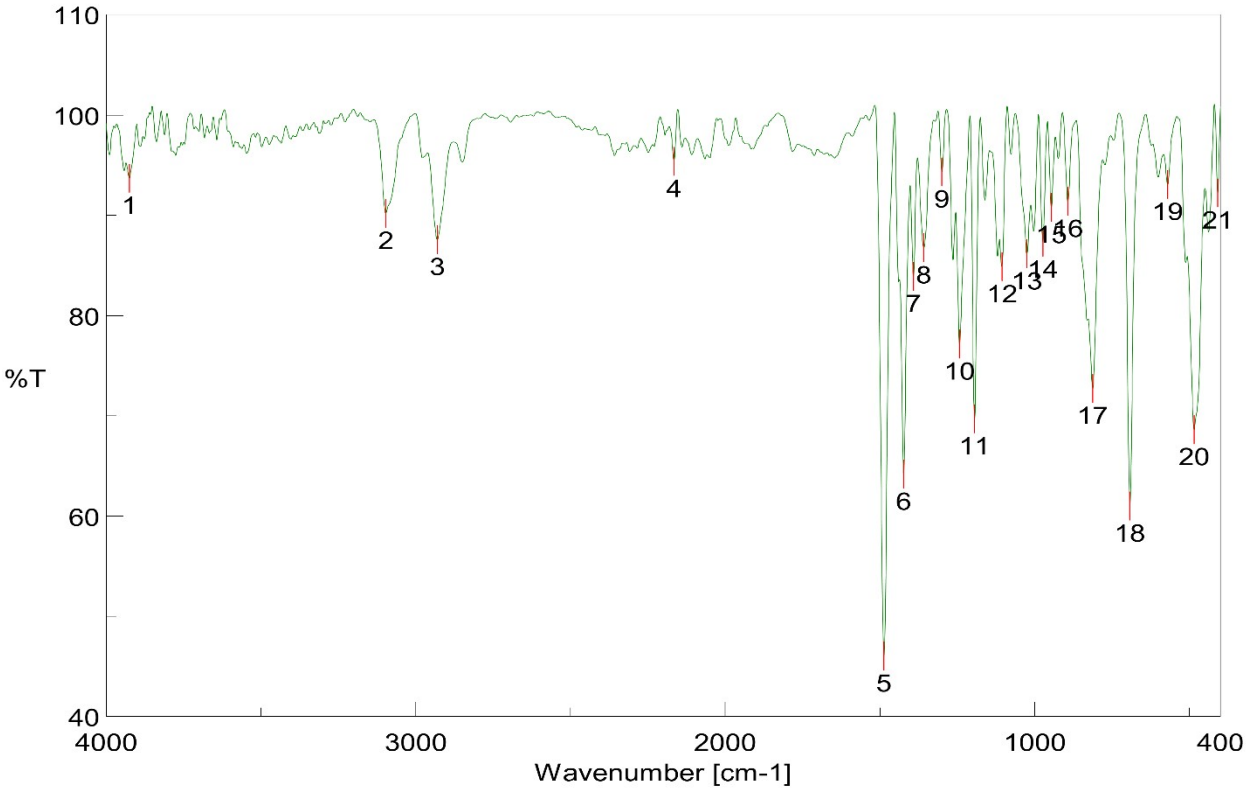


**Fig. S20.** FT-IR spectra of complex **6**.

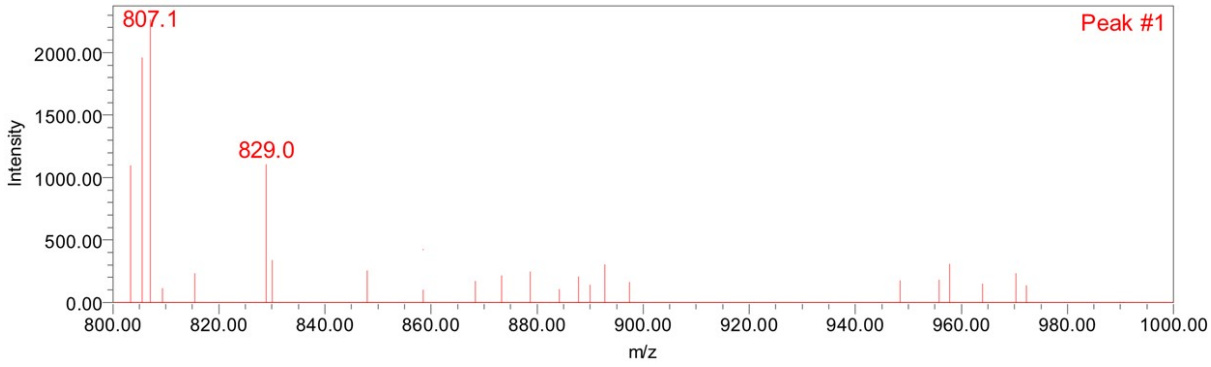


**Fig. S21.** ESI-MS spectra of complex **1**.

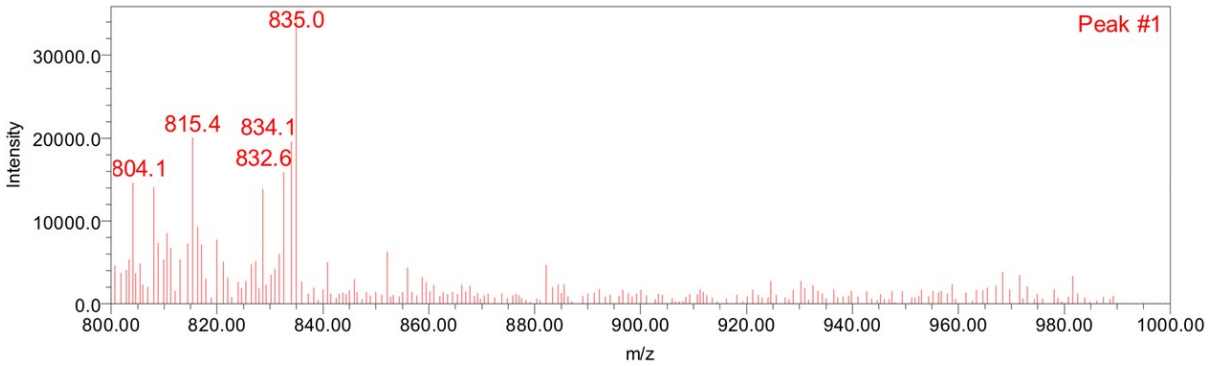


**Fig. S22.** ESI-MS spectra of complex **2**.

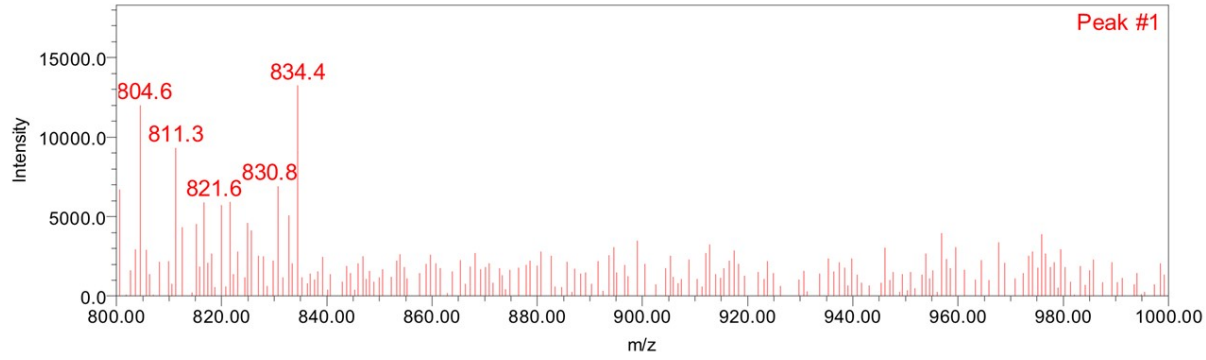


**Fig. S23.** ESI-MS spectra of complex **3**.

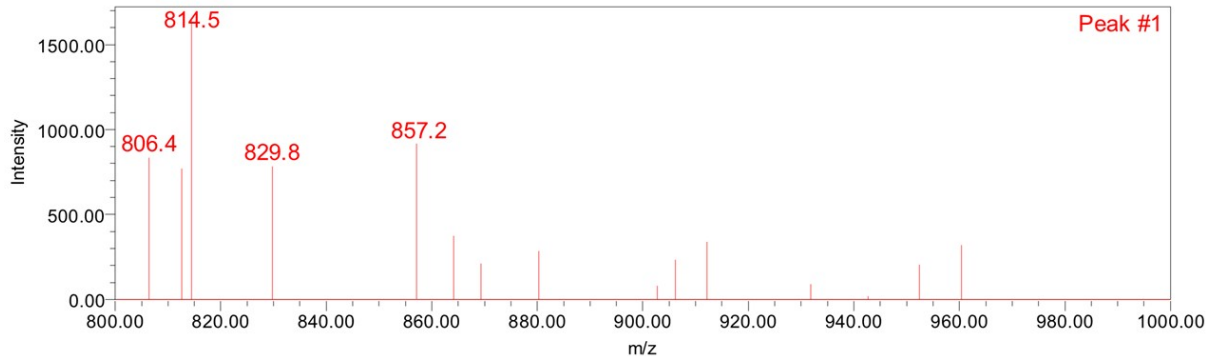


**Fig. S24.** ESI-MS spectra of complex **4**.

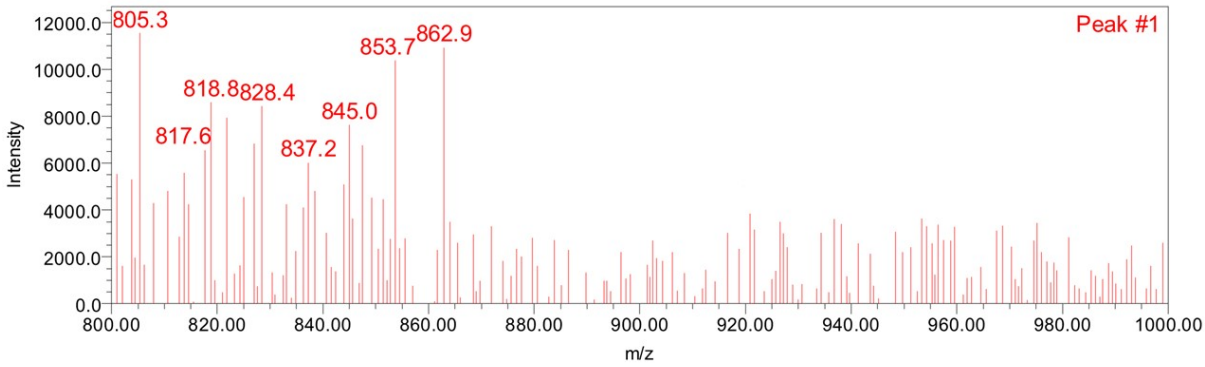


**Fig. S25.** ESI-MS spectra of complex **5**.

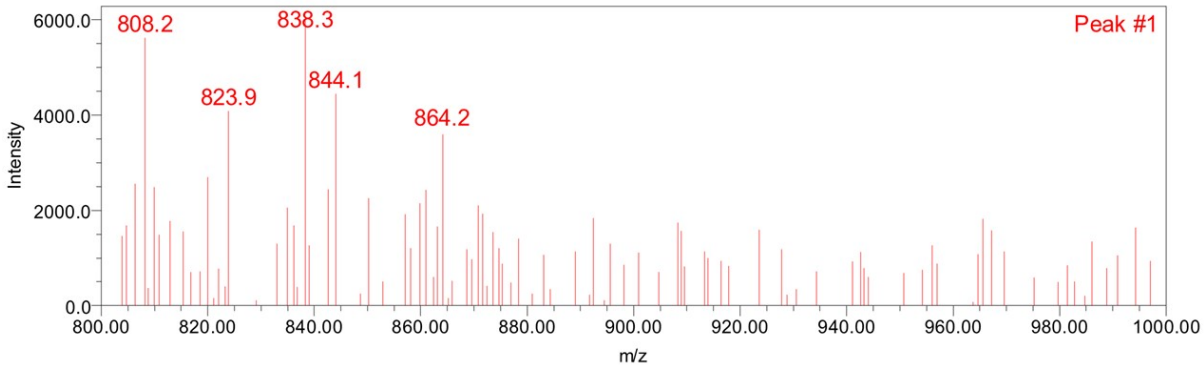


**Fig. S26.** ESI-MS spectra of complex **6**.

**Table S1.** UV-visible spectral data of ligand precursors and complexes **1-6** in $10^{-5}$ DCM.

| Entry | UV-vis spectral data ($10^{-5}$ DCM) $\lambda_{max}$ nm ($\varepsilon$ L mol$^{-1}$ cm$^{-1}$) | Wave Number (cm$^{-1}$) | Magnetic moment $\mu_{eff}$ (BM) |
|---|---|---|---|
| **L$^1$** | 272 (08535) ($\pi \rightarrow \pi^*$) | 36764 | - |
| | 306 (11321) ($n \rightarrow \pi^*$) | 32679 | |
| **L$^2$** | 270 (08338) ($\pi \rightarrow \pi^*$) | 37037 | - |
| | 318 (03586) ($n \rightarrow \pi^*$) | 31446 | |
| **1** | 278 (28414) ($\pi \rightarrow \pi^*$) | 35971 | dia |
| | 332 (60925) (n $\rightarrow \pi^*$) | 30120 | |
| | 394 (23557) charge transfer | 25380 | |
| | 612 (01204) d-d | 16339 | |
| **2** | 268 (63024) ($\pi \rightarrow \pi^*$) | 37313 | 1.79 |
| | 334 (05759) (n $\rightarrow \pi^*$) | 29940 | |
| | 436 (15283) charge transfer | 22935 | |
| | 616 (02014) d-d | 16233 | |
| **3** | 276 (68174) ($\pi \rightarrow \pi^*$) | 36231 | dia |
| | 324 (9135) (n $\rightarrow \pi^*$) | 30864 | |
| **4** | 270 (44459) ($\pi \rightarrow \pi^*$) | 37037 | dia |
| | 332 (120532) (n $\rightarrow \pi^*$) | 30120 | |
| | 398 (49608) charge transfer | 25125 | |
| | 608 (0809) d-d | 16447 | |
| **5** | 268 (114986) ($\pi \rightarrow \pi^*$) | 37313 | 1.78 |
| | 308 (106755) (n $\rightarrow \pi^*$) | 32467 | |
| | 434 (24588) charge transfer | 23041 | |
| | 618 (02059) d-d | 16181 | |
| **6** | 266 (195941) ($\pi \rightarrow \pi^*$) | 37593 | dia |
| | 310 (86146) (n $\rightarrow \pi^*$) | 32258 | |

**Table S2.** Summary of computational (DFT) data for complexes **1-6.**

| Code | Energy (Hartree) | HOMO (eV) | LUMO (eV) | Band Gap (eV) | Theoretical $\lambda_{max}$ value (nm) |
|---|---|---|---|---|---|
| 1 | -4229.70 | -5.650 | -2.272 | 3.378 | 370 |
| 2 | -4256.53 | -5.592 | -1.382 | 4.210 | 294 |
| 3 | -4125.99 | -5.642 | -2.297 | 3.345 | 288 |
| 4 | -4308.33 | -5.732 | -2.217 | 3.515 | 353 |
| 5 | -4335.17 | -5.524 | -1.289 | 4.235 | 293 |
| 6 | -4204.62 | -5.825 | -2.468 | 3.357 | 270 |

**Table S3.** Electrochemical parameters derived from the voltammograms for ligands **L[1]**-**L[2]** and complexes (**1**-**6**).

| Scan rate (mV/s) | $E_{p,a}$ (V) | $E_{p,c}$ (V) | $\Delta E = E_{p,a} - E_{p,c}$ (V) | $E^0 = (E_{p,a} + E_{p,c})/2$ (V) |
|---|---|---|---|---|
| | | **L[1]** | | |
| 50 | 1.088 | 0.222 | 0.866 | 0.655 |
| 100 | 1.219 | -0.051 | 1.270 | 0.584 |
| 150 | 1.352 | -0.158 | 1.510 | 0.597 |
| 200 | 1.413 | -0.234 | 1.647 | 0.589 |
| | | **1** | | |
| 50 | 0.830 | 0.555 | 0.275 | 0.692 |
| 100 | 0.896 | 0.464 | 0.432 | 0.680 |
| 150 | 0.937 | 0.435 | 0.502 | 0.686 |
| 200 | 0.979 | 0.401 | 0.578 | 0.690 |
| | | **2** | | |
| 50 | 1.040 | 0.316 | 0.724 | 0.678 |
| 100 | 1.287 | -0.033 | 1.320 | 0.627 |
| 150 | 1.362 | -0.099 | 1.461 | 0.631 |
| 200 | 1.369 | -0.081 | 1.450 | 0.644 |
| | | **3** | | |
| 50 | 1.030 | 0.377 | 0.653 | 0.703 |
| 100 | 1.213 | 0.214 | 0.999 | 0.713 |
| 150 | 1.245 | 0.089 | 1.156 | 0.667 |
| 200 | 1.194 | -0.149 | 1.343 | 0.522 |
| | | **L[2]** | | |
| 50 | 0.981 | 0.144 | 0.837 | 0.562 |
| 100 | 1.117 | 0.009 | 1.108 | 0.563 |
| 150 | 1.201 | -0.071 | 1.272 | 0.565 |
| 200 | 1.272 | -0.126 | 1.398 | 0.699 |
| | | **4** | | |
| 50 | 0.871 | 0.578 | 0.293 | 0.724 |
| 100 | 0.624 | 0.361 | 0.263 | 0.492 |
| 150 | 0.604 | 0.348 | 0.256 | 0.476 |
| 200 | 0.557 | 0.329 | 0.228 | 0.443 |
| | | **5** | | |
| 50 | 1.180 | -0.016 | 1.196 | 0.582 |
| 100 | 1.342 | -0.310 | 1.652 | 0.516 |
| 150 | 1.374 | -0.387 | 1.761 | 0.493 |
| 200 | 1.288 | -0.442 | 1.730 | 0.423 |
| | | **6** | | |
| 50 | 0.746 | 0.426 | 0.320 | 0.586 |
| 100 | 0.774 | 0.394 | 0.380 | 0.584 |
| 150 | 0.858 | 0.366 | 0.492 | 0.612 |
| 200 | 0.911 | 0.330 | 0.581 | 0.620 |

**Table S4.** Thermogravimetric data of dithiocarbamate metal complexes **1-6**.

| Entry | Steps | Temp. | Weight loss on TGA (%) | DTA peak (°C) | Inference |
|---|---|---|---|---|---|
| 1 | I | 243-579 | 50.0 | 244.0 | Mass loss continues even after 800 °C. |
| 2 | I | 41-94 | 8.0 | - | Mass loss continues even after 800 °C. |
| | II | 95-428 | 54.0 | 183.0 | |
| 3 | I | 200-337 | 27.0 | 205.0 | Mass loss continues even after 800 °C. |
| | II | 338-480 | 6.0 | - | |
| 4 | I | 248-433 | 67.0 | 256.3 | Mass loss continues even after 800 °C. |
| 5 | I | 185-448 | 66.0 | 203.0 | Mass loss continues even after 800 °C. |
| 6 | I | 229-454 | 66.0 | 261.7 | Mass loss continues even after 800 °C. |

**Table S5.** Antiproliferative activity ($GI_{50}$, μM) against human cancer cell lines of synthesized ligands **$L^1$**, **$L^2$,** and compounds **1-6**.

| Compound | Antiproliferative activity ($GI_{50}$)[a] | | | | | |
|---|---|---|---|---|---|---|
| | Cell line (origin) | | | | | |
| | A549 (lung) | HeLa (cervix) | MIA PaCa-2 (pancreas) | SW1573 (lung) | T-47D (breast) | WiDr (colon) |
| **$L^1$** | 42 ± 13 | 22 ± 4.8 | >100 | 88 ± 21 | 74 ± 29 | 52 ± 20 |
| **$L^2$** | 83 ± 24 | 40 ± 7.5 | 77 ± 34 | 78 ± 33 | 30 ± 5.2 | 37 ± 6.5 |
| **1** | >100 | >100 | >100 | >100 | >100 | >100 |
| **2** | >100 | >100 | >100 | >100 | >100 | >100 |
| **3** | 12 ± 3.2 | 7.7 ± 0.74 | 7.5 ± 0.62 | 5.3 ± 1.1 | 66 ± 19 | 37 ± 13 |
| **4** | >100 | >100 | >100 | >100 | >100 | >100 |
| **5** | >100 | >100 | >100 | >100 | >100 | >100 |
| **6** | 11 ± 1.7 | 5.2 ± 0.62 | 7.5 ± 2.3 | 5.8 ± 0.07 | >100 | >100 |
| **CDDP** [c] | 4.9 ± 0.2 | 1.8 ± 0.5 | n.d. | 2.7 ± 0.4 | 17 ± 3.3 | 23 ± 4.3 |
| **5-FU** [c] | 2.2 ± 0.3 | 16 ± 4.5 | n.d. | 3.3 ± 1.2 | 43 ± 16 | 49 ± 6.7 |

Values represent mean ± standard deviation of at least three independent experiments. n.d. = not determined.

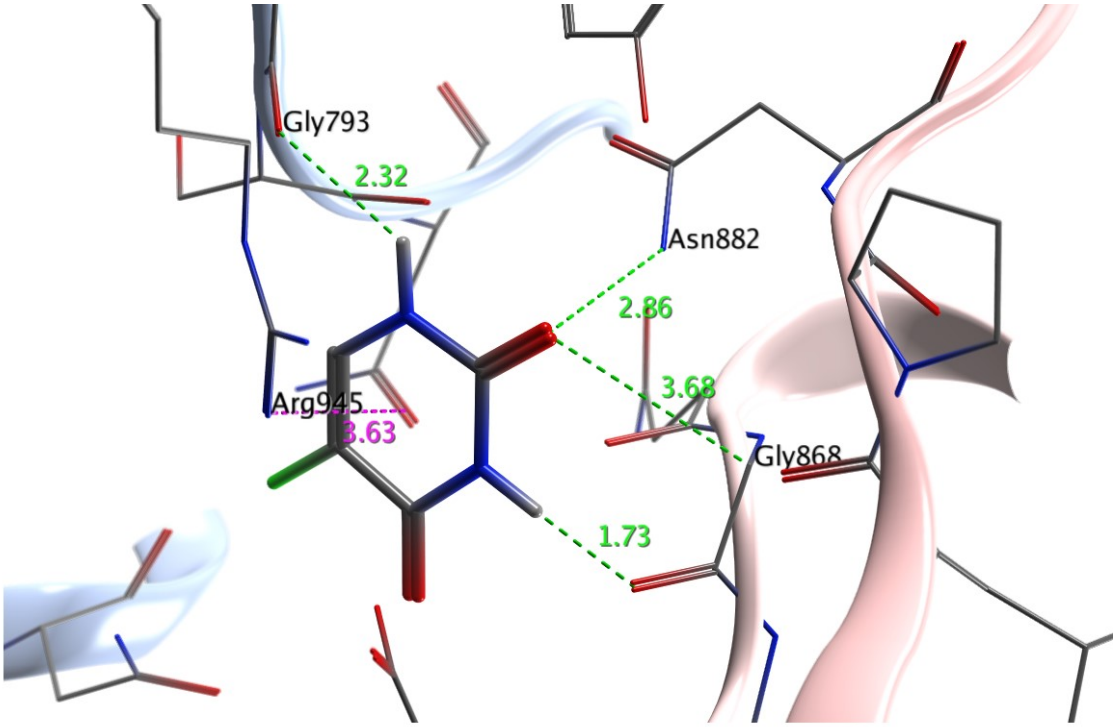


**Fig. S27.** Molecular docking studies of 5-fluorouracil (5-FU) with human topoisomerase II beta in complex with DNA (PDB ID: 3qx3).

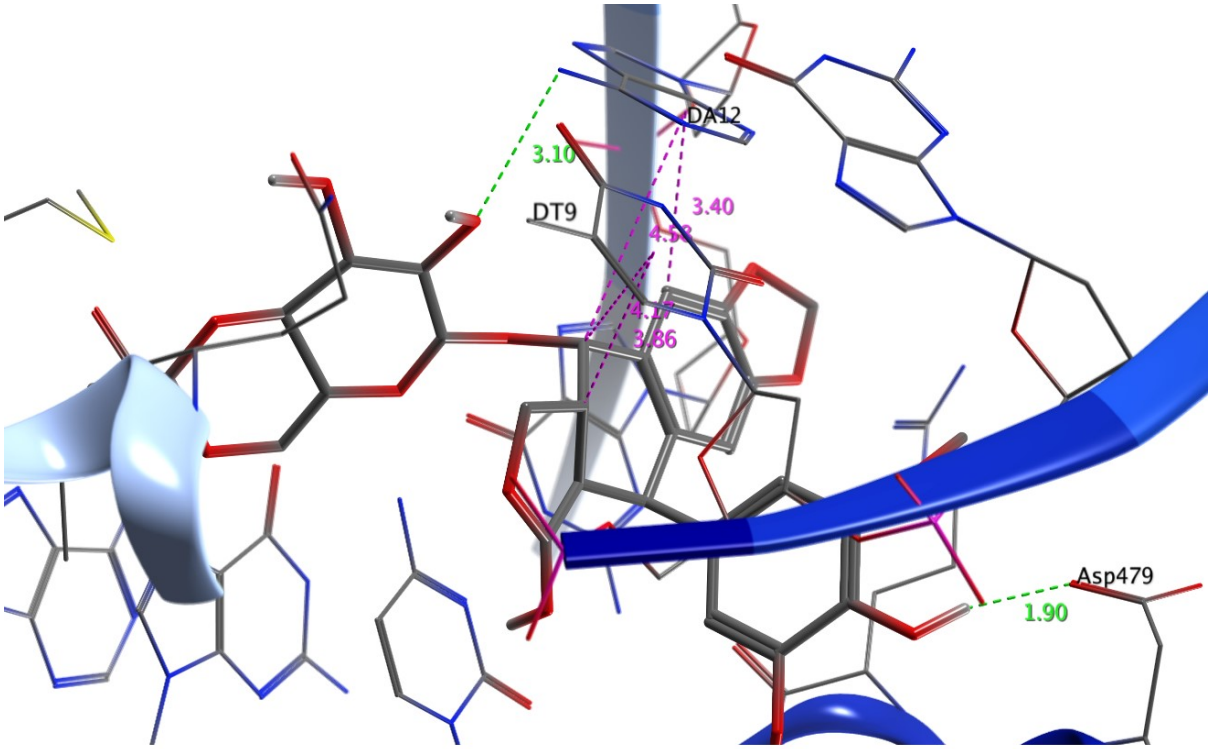


**Fig. S28.** Molecular docking studies of co-ligand (native) with human topoisomerase II beta in complex with DNA (PDB ID: 3qx3).

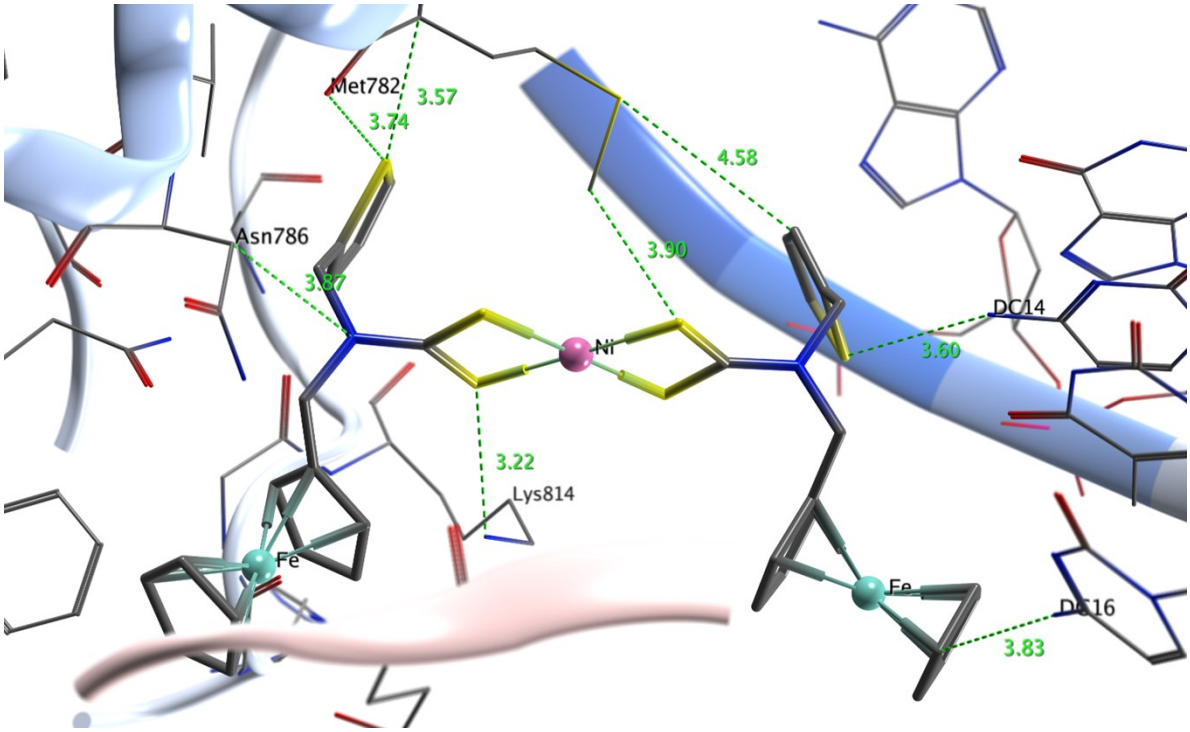


**Fig. S29.** Molecular docking studies of complex **1** with human topoisomerase II beta in complex with DNA (PDB ID: 3qx3).

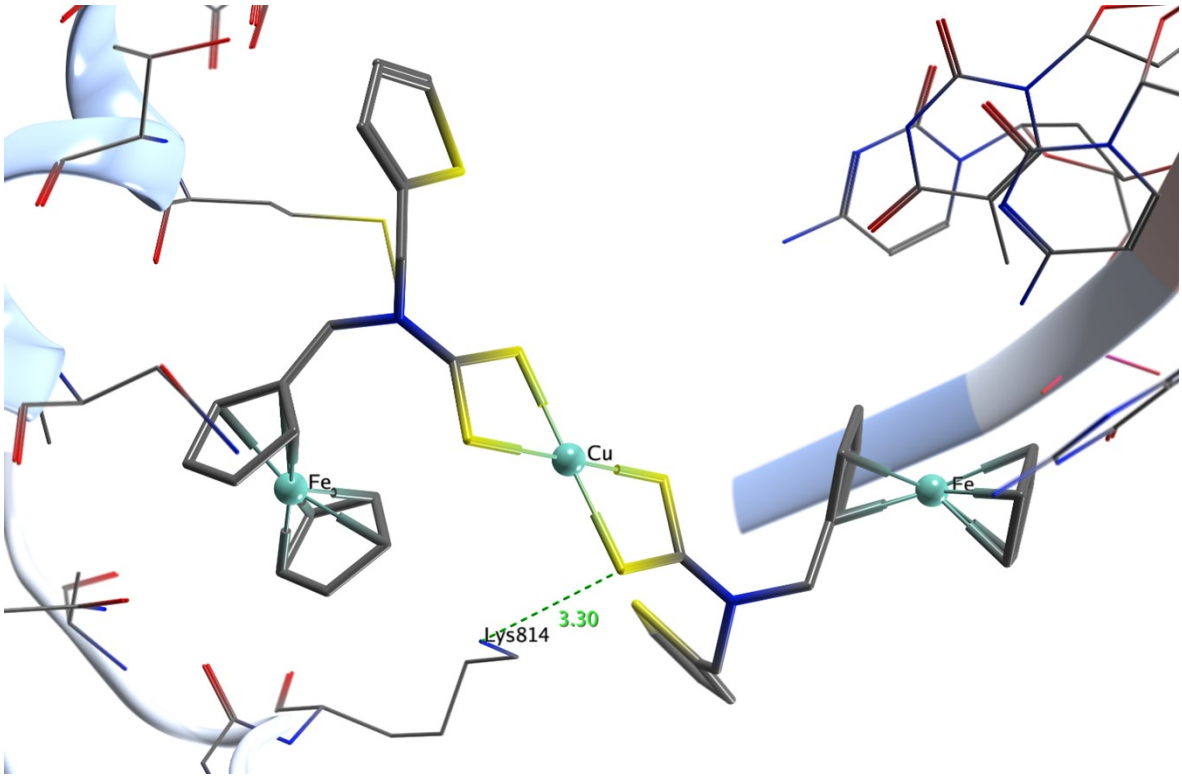


**Fig. S30.** Molecular docking studies of complex **2** with human topoisomerase II beta in complex with DNA (PDB ID: 3qx3).

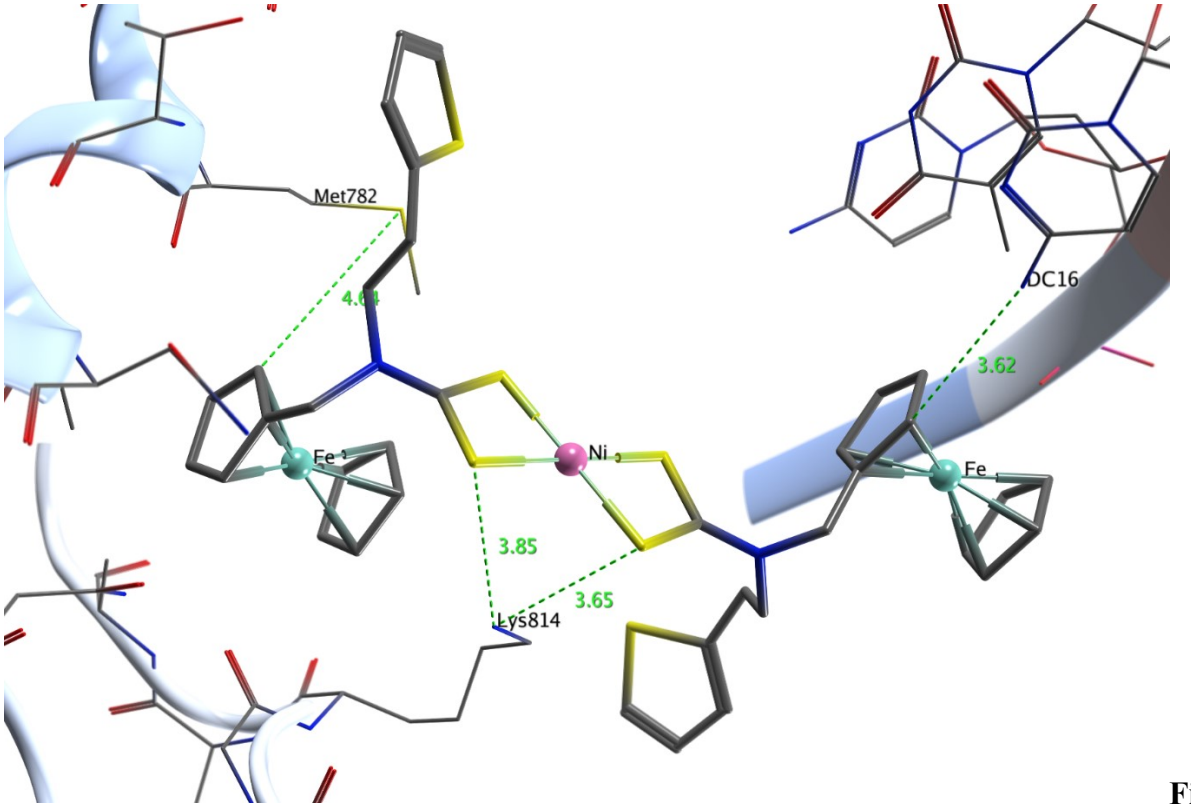


**Fi**

**g. S31.** Molecular docking studies of complex **4** with human topoisomerase II beta in complex with DNA (PDB ID: 3qx3).

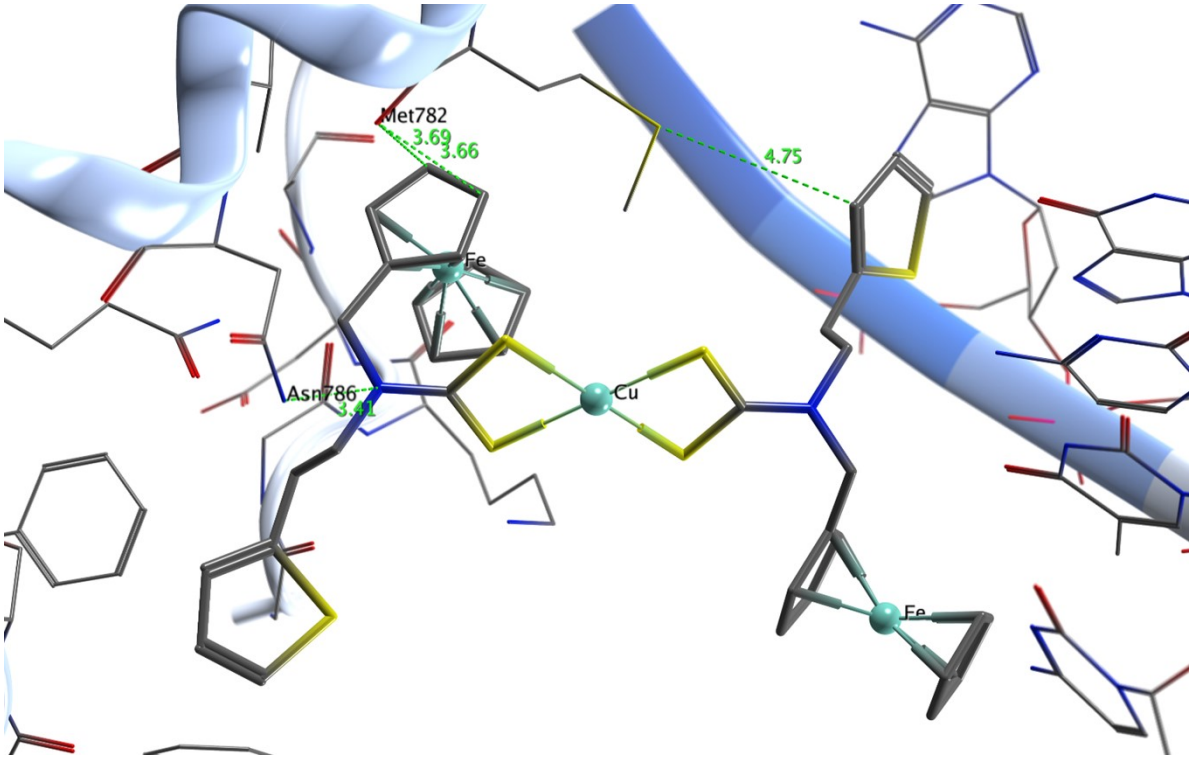


**Fig. S32.** Molecular docking studies of complex **5** with human topoisomerase II beta in complex with DNA (PDB ID: 3qx3).

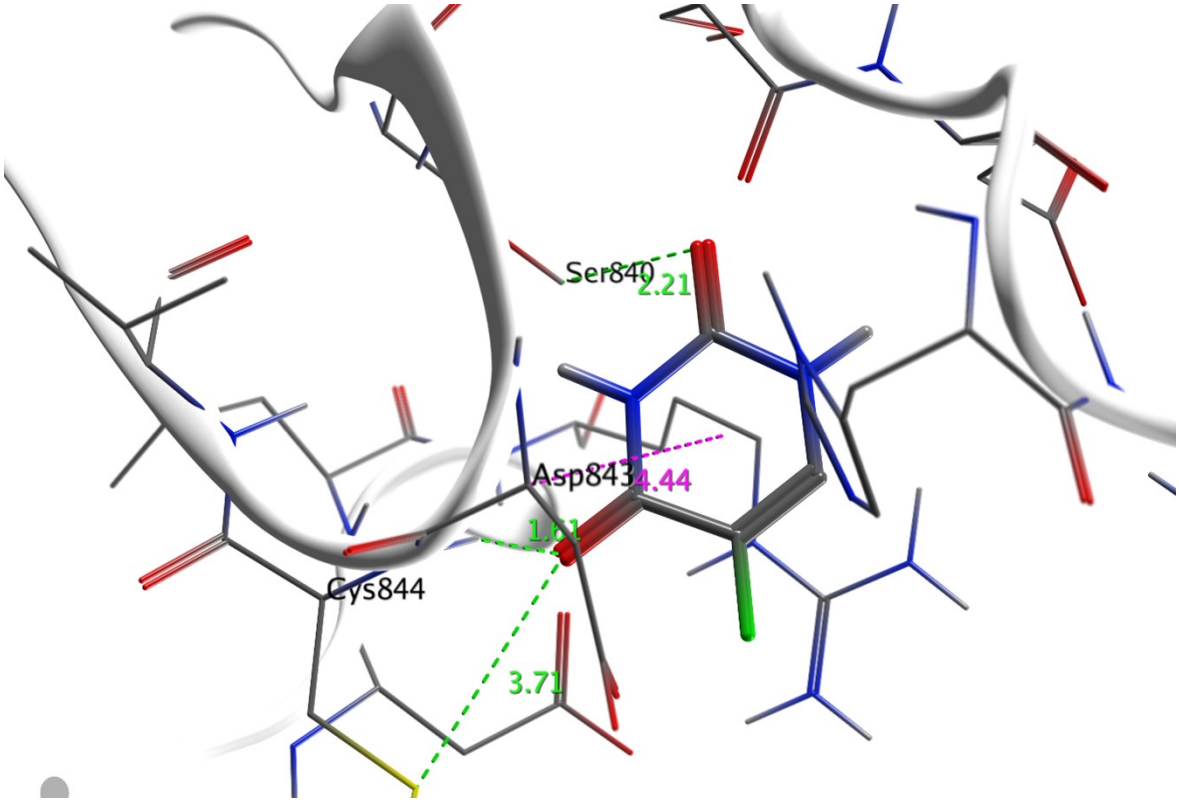


**Fig. S33.** Molecular docking studies of 5-fluorouracil (5-FU) with protein PI3Kα (PDB ID: 4jps).

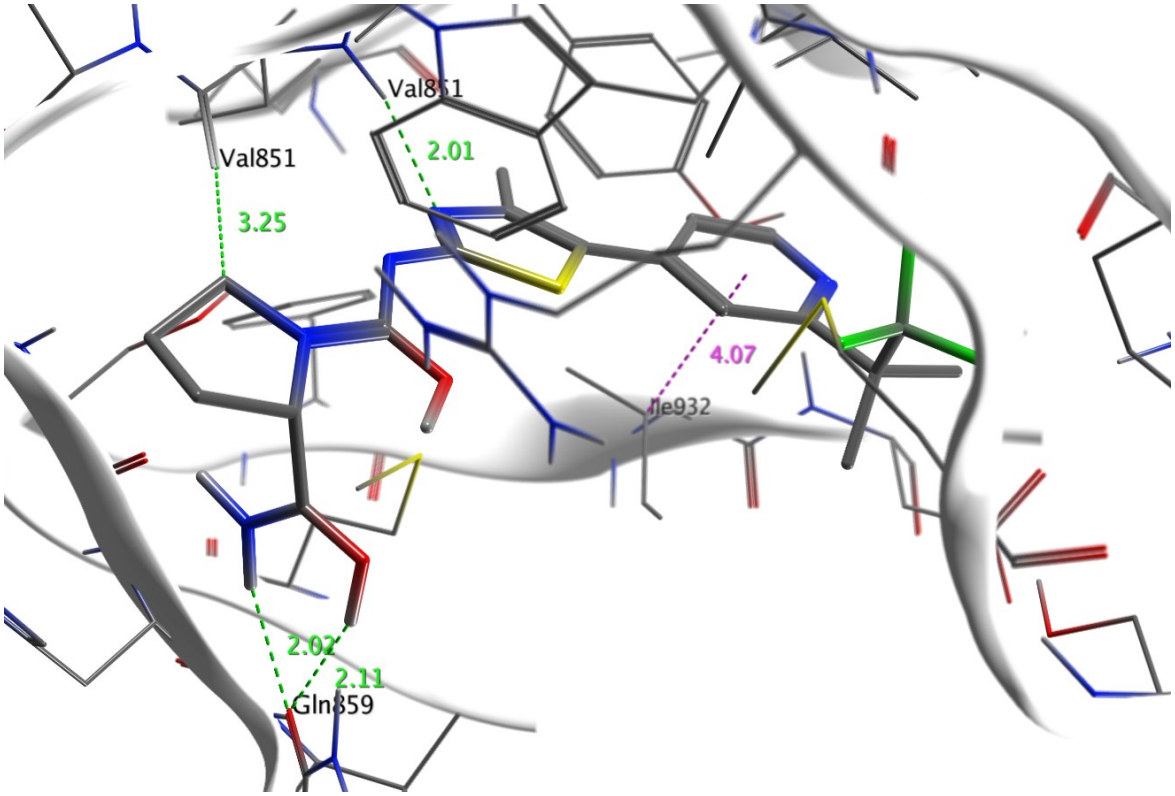


**Fig. S34.** Molecular docking studies of co-ligand (native) with protein PI3Kα (PDB ID: 4jps).

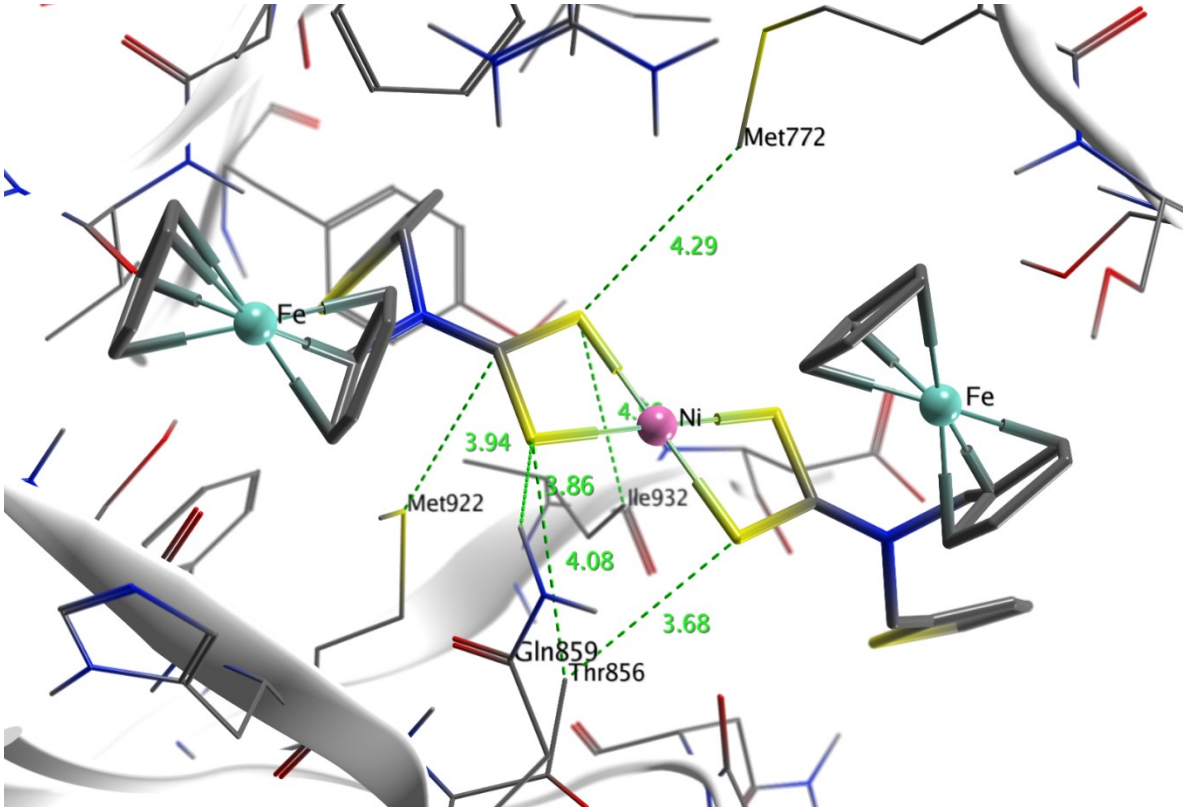


**Fig. S35.** Molecular docking studies of complex **1** with protein PI3Kα (PDB ID: 4jps).

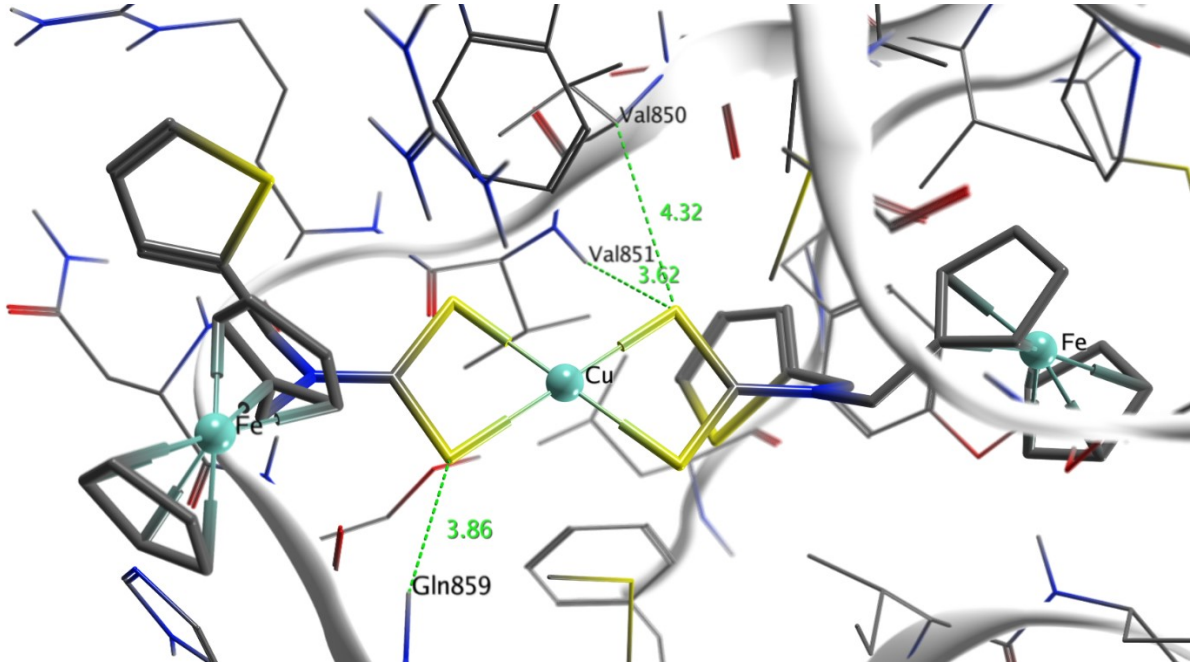


**Fig. S36.** Molecular docking studies of complex **2** with protein PI3Kα (PDB ID: 4jps).

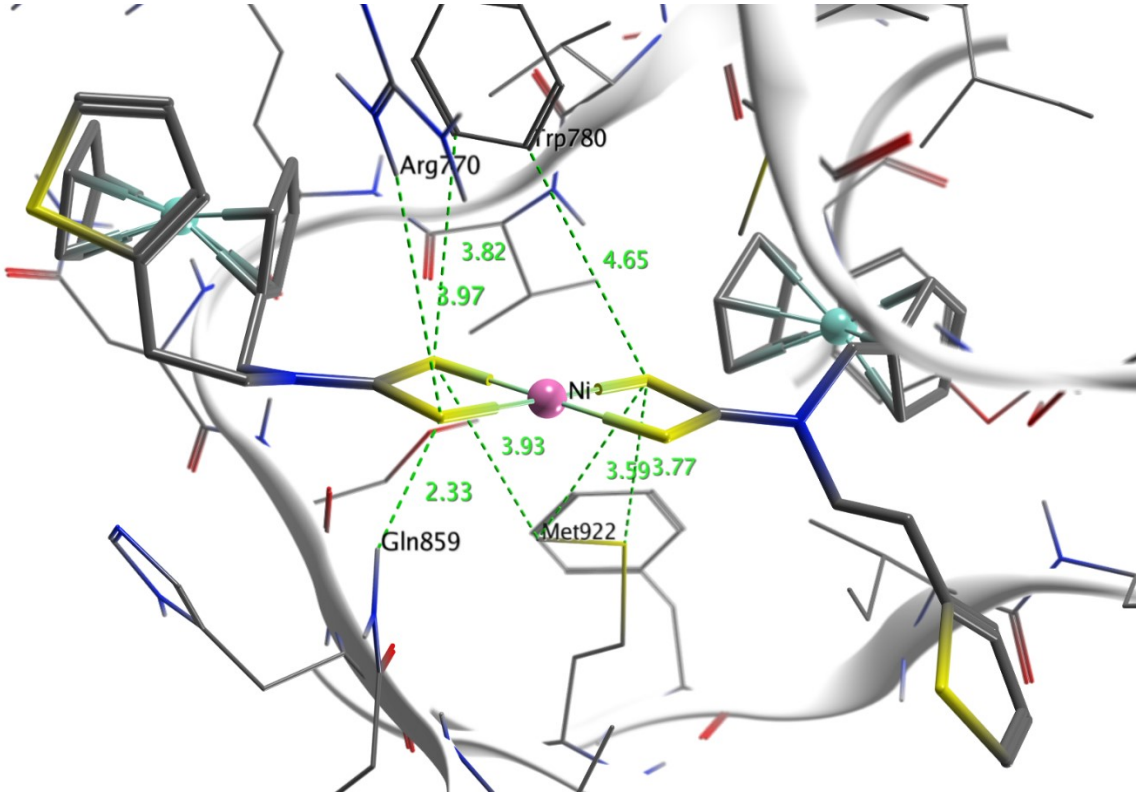


**Fig. S37.** Molecular docking studies of complex **4** with protein PI3Kα (PDB ID: 4jps).

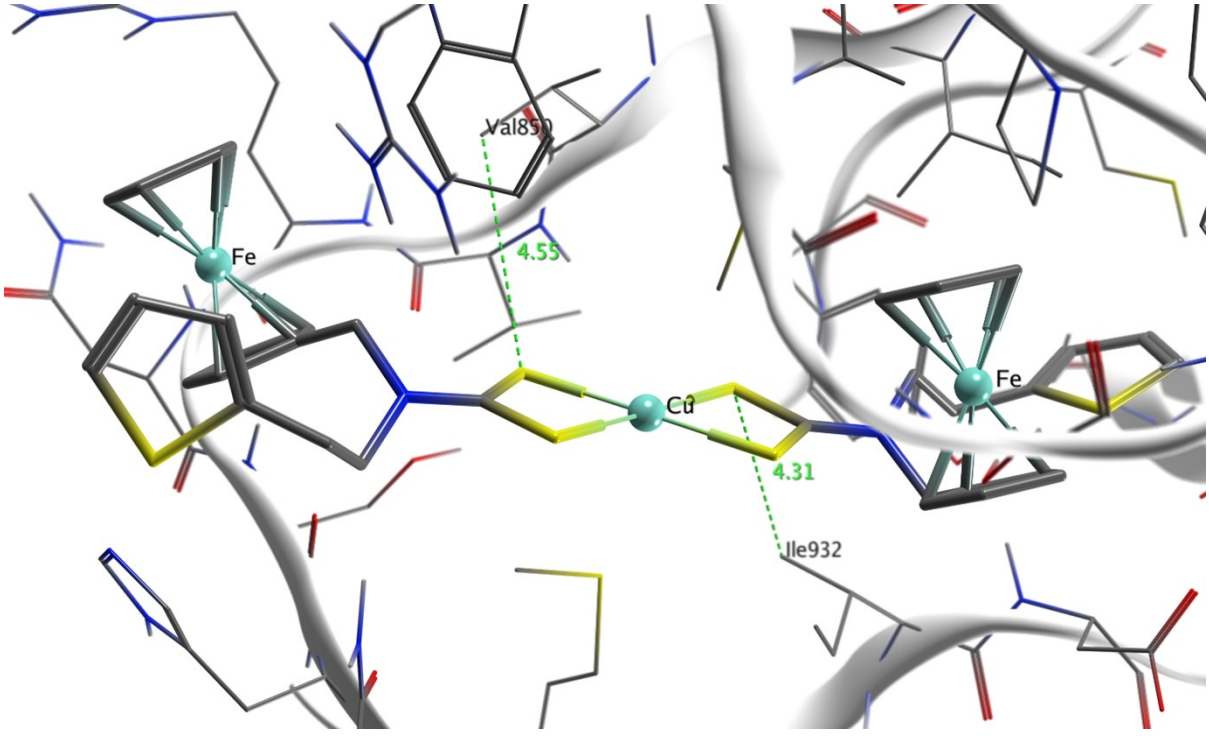


**Fig. S38.** Molecular docking studies of complex **5** with protein PI3Kα (PDB ID: 4jps).